Karlsruhe Institute of Technology

wave phenomena
analysis and numerics

Error analysis of second-order local time integration methods for discontinuous Galerkin discretizations of linear wave equations

Constantin Carle, Marlis Hochbruck

CRC Preprint 2023/2 (revised), May 2023

KARLSRUHE INSTITUTE OF TECHNOLOGY

CRC 1173

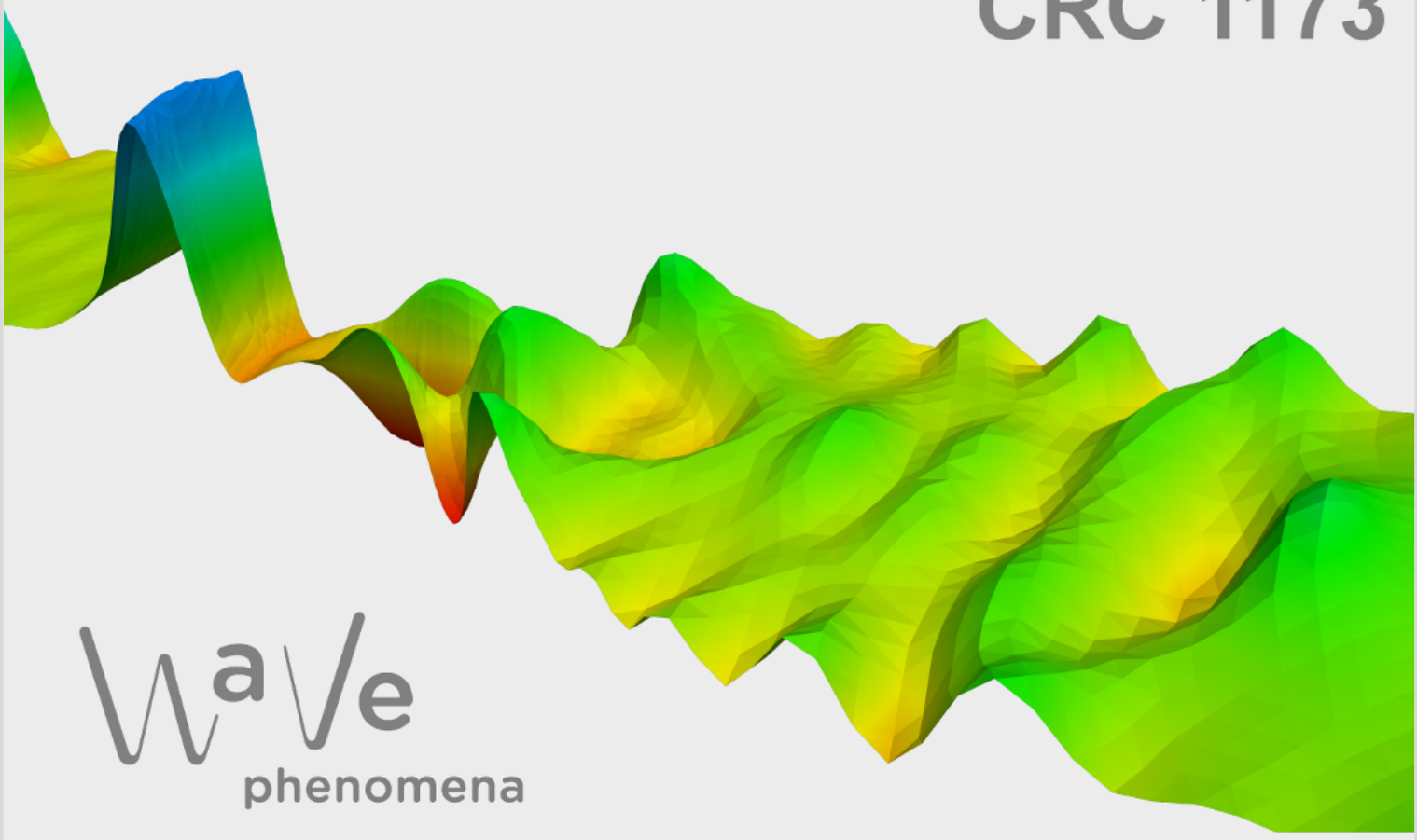

Participating universities

Universität Stuttgart

EBERHARD KARLS
UNIVERSITÄT
TÜBINGEN

Funded by

ISSN 2365-662X

ERROR ANALYSIS OF SECOND-ORDER LOCAL TIME INTEGRATION METHODS FOR DISCONTINUOUS GALERKIN DISCRETIZATIONS OF LINEAR WAVE EQUATIONS

CONSTANTIN CARLE AND MARLIS HOCHBRUCK

Abstract. This paper is dedicated to the full discretization of linear wave equations, where the space discretization is carried out with a discontinuous Galerkin method on spatial meshes which are locally refined or have a large wave speed on only a small part of the mesh. Such small local structures lead to a strong CFL condition in explicit time integration schemes causing a severe loss in efficiency. For these problems, various local time-stepping schemes have been proposed in the literature in the last years and have been shown to be very efficient. Here, we construct a quite general class of local time integration methods preserving a perturbed energy and containing local time-stepping and locally implicit methods as special cases. For these two variants we prove stability and optimal convergence rates in space and time. Numerical results confirm the stability behavior and show the proved convergence rates.

1. Introduction

In this paper we consider the discretization of linear acoustic wave equations in space and time by a methods of lines approach. For the space discretization, a popular choice is to apply discontinuous Galerkin (dG) methods, since they allow one to handle heterogeneous or complex materials by using unstructured meshes, cf. [18, 30]. At the cost of a larger number of degrees of freedom compared to conforming finite element methods, a main advantage is that dG methods lead to block diagonal mass matrices. In combination with an explicit time integrator, this yields a fully explicit scheme.

Unfortunately, the system of ordinary differential equations (ODEs) resulting from (any kind of) spatial discretization is stiff and thus explicit schemes suffer from stability issues caused by a strong CFL condition. Roughly speaking, if we define a local CFL parameter ξ_K as the quotient of the wave speed and the diameter of a mesh element K, then the time-step size τ must fulfill $\tau \max_K \xi_K \lesssim 1$ for stability. Large values of ξ_K are caused by a large wave speed or a small diameter of K. Even if we have a large ξ_K only on a single element K, this leads to a strong CFL condition meaning that an explicit scheme has to use a very small time-step size on all elements. Hence, explicit methods perform poorly if we have a large CFL parameter (and thus a strong CFL condition) on only a few elements but a

2020 *Mathematics Subject Classification.* Primary 65M12, 65M15, 65M22; Secondary 65M20, 65M60.

Key words and phrases. time integration, wave equation, leapfrog method, discontinuous Galerkin method, error analysis, CFL condition, Chebyshev polynomials, local time-stepping, locally implicit.

Funded by the Deutsche Forschungsgemeinschaft (DFG, German Research Foundation) – Project-ID 258734477 – SFB 1173.

large number of elements with a small or moderate CFL parameter (which require a weak CFL condition). Such situations appear in many applications. For instance, locally refined meshes might be necessary to resolve small-scale geometric features or if the exact solution locally lacks regularity (corner singularities). In [45], it was shown that the solution remains smooth over time in a certain distance away from the corner and that graded meshes yield optimal convergence rates of the finite element discretization.

An alternative to explicit schemes are implicit methods such as the Crank–Nicolson (implicit trapezoidal) scheme. The advantage of these methods is that they are unconditionally stable. This means that the time-step size is only restricted by the accuracy of the approximation but not by stability. The disadvantage is that implicit methods require the solution of a large linear systems of equations, which might be unfeasible for problems in three space dimensions.

As a remedy, two variants of local time integration schemes have been proposed: local time-stepping (LTS) and locally implicit methods. LTS methods for wave equations are constructed in, e.g., [3, 19, 20, 26, 28, 29], and for Maxwell's equations in [27, 40, 44, 48]; see also references therein. Locally implicit schemes have only been considered for Maxwell's equations, see, e.g., [14, 15, 16, 21, 36, 37, 49, 52]. These schemes use an explicit scheme, e.g., the leapfrog (Verlet) method, on the elements with a small value of ξ_K and either an implicit or an explicit scheme with a more favorable CFL condition on the few remaining elements. A related approach, where two explicit solvers are coupled with a Lagrange multiplier on the interface between the two submeshes is presented in [9, 11, 12, 38]. These methods require the solution of a linear system for the Lagrange multiplier in each time step, whose dimension is much smaller than for locally implicit or fully implicit methods.

To the best of our knowledge there are only a few papers containing rigorous error bounds: locally implicit methods for Maxwell's equations in [36, 37] and [25] for LTS for the linear, homogeneous wave equation. In [25], a modification of the very efficient and popular scheme proposed in [19] was analyzed for finite element space discretization combined with mass lumping. This modification was motivated by our earlier work [7, 8] on second-order ODEs. For the related approach using Lagrange multipliers, a rigorous analysis is given in [9].

In contrast to the existing literature on local time integration schemes we consider a quite general class of methods which contains LTS and locally implicit methods as special cases. The LTS schemes use the leapfrog method on those elements with a weak local CFL condition and the explicit leapfrog-Chebyshev (LFC) method [8], which are based on stabilized Chebyshev polynomials, on the remaining elements. To ensure stability under the weak local CFL condition, the degree of these polynomials and the stabilization parameter have to be chosen appropriately. For LTS schemes, the coupling between the elements treated by the leapfrog and the LFC scheme, respectively, enter the CFL condition. Our analysis is based on [7, 8]. It differs from the recent work in [25] in the considered space discretization: we study a dG method while in [25] finite elements with mass lumping are studied. In addition, compared to [25] we could weaken the CFL condition, require less regularity of the solution, and include inhomogeneities.

We are not aware of any rigorous results for locally implicit schemes so far for wave equations. Our new result is a proof that this scheme is stable if the leapfrog scheme on the elements with a small CFL parameter is stable. Hence, in contrast

to LTS methods, the stability is independent of the coupling. For both, LTS and locally implicit methods, we prove error bounds of optimal order in space and time under regularity assumptions on the solution which correspond to the ones required for the leapfrog or θ-scheme in [32, 39].

Outline. We start in Section 2 by setting the analytical framework for the forthcoming presentation. The construction of a general class of local time integration methods for the linear wave equation is presented in Section 3, where we also state the main results of our paper. A review of the *symmetric weighted interior penalty* discontinuous Galerkin method for the wave equation is given in Section 4. In Section 5 we shortly investigate the stability and energy conservation of the general scheme and state CFL conditions for the special cases of LTS and locally implicit schemes. A crucial result is that these conditions only depend on the elements with a small CFL parameter ξ_K. For LTS methods, which are fully explicit, this holds if the polynomial degree and the stabilization parameter used within the LFC scheme are chosen appropriately. Here, we benefit from our results in [7]. Afterwards, in Section 6, we perform the error analysis showing error bounds of optimal order for the LTS and locally implicit scheme. Finally, we confirm our theoretical findings with some numerical examples in Section 7.

2. Analytic setting

In this section we shortly present the analytic setting. Let $\Omega \subset \mathbb{R}^d$, $d = 1, 2, 3$, be a bounded Lipschitz domain. For a set $K \subseteq \Omega$ and $u \in L^2(K)$ sufficiently regular, say $H^1(\Omega)$, we denote the $L^2(K)$-norm and the $L^2(F)$-norm, $F \subset \partial K$, by

$$\|u\|_K^2 = \int_K u(x)^2 \,\mathrm{d}x, \qquad \|u\|_F^2 = \int_F (u(x)|_F)^2 \,\mathrm{d}\sigma,$$

respectively. Whenever it is clear from the context, we abbreviate $\|\cdot\| = \|\cdot\|_\Omega$. Analogous definitions hold for vector fields $U \in L^2(\Omega)^d$.

For a partition $\mathcal{B}$ of Ω into finite disjoint Lipschitz subdomains, we denote by

$$H^r(\mathcal{B}) = \big\{ v \in L^2(\Omega) \mid v|_B \in H^r(B) \text{ for all } B \in \mathcal{B} \big\}, \qquad r \geq 0,$$

piecewise/broken fractional Sobolev spaces fitting the partition $\mathcal{B}$. Here, we define fractional Sobolev spaces $H^r(B)$ via Sobolev-Slobodeckij spaces or real interpolation spaces; see, e.g., [2, 17, 51] for more information. For the norm and seminorm of the Hilbert spaces $H^r(\mathcal{B})$ we write

$$\|v\|_{r,\mathcal{B}}^2 = \sum_{B \in \mathcal{B}} \|v\|_{r,B}^2, \qquad |v|_{r,\mathcal{B}}^2 = \sum_{B \in \mathcal{B}} |v|_{r,B}^2,$$

where $\|v\|_{r,B}$ and $|v|_{r,B}$ denote the norm and seminorm of $H^r(B)$, respectively.

For a finite time $T > 0$ we consider the linear acoustic wave equation

$$\partial_t^2 u = \nabla \cdot (\kappa \nabla u) + f \qquad \text{in } (0,T) \times \Omega, \tag{2.1a}$$

subject to homogeneous Dirichlet boundary conditions and initial conditions

$$u = 0 \qquad \text{on } (0,T) \times \partial\Omega, \tag{2.1b}$$

$$u(0) = u^0, \quad \partial_t u(0) = v^0 \qquad \text{in } (0,T) \times \Omega. \tag{2.1c}$$

By $f \colon (0,T) \times \Omega \to \mathbb{R}$ we denote a given source term. We assume that the wave speed $\kappa^{1/2} : \overline{\Omega} \to \mathbb{R}_+$ is piecewise smooth and uniformly bounded, i.e.,

$$0 < \kappa_{\min} \leq \kappa(x) \leq \kappa_{\max} < \infty \qquad \text{for all } x \in \overline{\Omega}. \tag{2.2}$$

We point out that the restriction to homogeneous Dirichlet boundary conditions is only for the sake of presentation. The following results can be transferred to other boundary conditions and even extended to other second-order problems, e.g., Maxwell's equations; see Section 6.3 for more details.

The acoustic wave equation (2.1) is a special case of a second-order evolution equation

$$\partial_t^2 u = -Au + f \qquad \text{in } L^2(\Omega), \tag{2.3a}$$

$$u(0) = u^0, \quad \partial_t u(0) = v^0, \tag{2.3b}$$

with $A\colon D(A) \to L^2(\Omega)$ defined via

$$Au = -\nabla \cdot (\kappa \nabla u)$$

on its domain $D(A) = H_0^1(\Omega) \cap \{u \in L^2(\Omega) \mid \nabla \cdot (\kappa \nabla u) \in L^2(\Omega)\}$. It is well-known that A is self-adjoint on $L^2(\Omega)$ and coercive on $H_0^1(\Omega)$. Moreover, the following result holds; see, e.g., [34, Theorem 4.3].

Lemma 2.1. *Let $u^0 \in D(A)$, $v^0 \in H_0^1(\Omega)$ and $f \in C(0,T;D(A)) + C^1(0,T;L^2(\Omega))$. Then, the exact solution of (2.1) satisfies*

$$u \in C(0,T;D(A)) \cap C^1(0,T;H_0^1(\Omega)) \cap C^2(0,T;L^2(\Omega)).$$

Additional to the above conditions we make further assumptions on the domain Ω and the material parameter κ to simplify the representation and the proofs for the error estimate of the space discretization. A definition of a polyhedron in $\mathbb{R}^d$ is given in [18, Definition 1.6], for instance.

Assumption 2.2. *Let Ω be a Lipschitz polyhedron in $\mathbb{R}^d$. Further, there exists a partition P_Ω of Ω into $N_\Omega \in \mathbb{N}$ disjoint Lipschitz polyhedra Ω_i, $i \in \{1,\dots,N_\Omega\}$ such that $\kappa|_{\Omega_i}$ is constant for all $i \in \{1,\dots,N_\Omega\}$.*

These assumptions enable us to cover the domain Ω and its subdomains exactly with a mesh. Moreover, the evaluation of κ causes no additional quadrature errors. Nevertheless, we expect that the following analysis can be extended to these cases with additional technical effort; see, e.g., [34, 35] how to deal with such additional approximations.

Moreover, since we are interested in error bounds of u in $L^2(\Omega)$, we require *elliptic regularity* for optimal error bounds (recall that A is self-adjoint).

Assumption 2.3. *Let $\mu > \frac{1}{2}$. There is a constant $c_{\mathrm{ell}} = c_{\mathrm{ell}}(\Omega,\mu)$ such that for all $f \in L^2(\Omega)$ the solution $z \in D(A)$ of the problem*

$$Az = f$$

belongs to $z \in D(A) \cap H^{1+\mu}(P_\Omega)$ and satisfies $\|z\|_{1+\mu,P_\Omega} \le c_{\mathrm{ell}}\|f\|$.

We emphasize that we do not assume $z \in H^{1+\mu}(\Omega)$ for a $\mu > \frac{1}{2}$ which is clearly wrong for the case of piecewise constant κ (to obtain such a regularity one requires at least Lipschitz continuity of κ on $\overline{\Omega}$). Although even $z \in H^{1+\mu}(P_\Omega)$ for $\mu > \frac{1}{2}$ does not hold in general, there are cases for piecewise constant κ such that the above regularity holds; see, e.g., [13, 46, 47]. Moreover, in the case of constant κ on general Lipschitz domains (e.g., non-convex polygonal domains) one always obtains $H^{3/2+\varepsilon}(\Omega)$ for some $\varepsilon > 0$; see, e.g., [24, Section 31.4] and references therein.

In the following, we let Assumptions 2.2 and 2.3 hold without mentioned explicitly everywhere.

For the subsequent analysis, we assume a slightly more regular solution in space than in Lemma 2.1. Based on the previous assumption we introduce for a $\mu > \frac{1}{2}$ the space

$$V_\star = D(A) \cap H^{1+\mu}(P_\Omega). \tag{2.4}$$

This allows for well-defined traces in L^2 for $\kappa\nabla u$. We expect that the subsequent analysis can be extended to the case $V_\star = D(A)\cap H^{1+\mu}(P_\Omega)$, $\mu > 0$. However, since in this case $(n \cdot \kappa\nabla u)|_\Gamma \in H^{-1/2}(\Gamma)$ for $\Gamma \subset \partial\Omega_i, \Omega_i \in P_\Omega$, the analysis becomes more involved and technical; see [24, Chapter 41] for details how this can be done.

After setting the analytical framework, the next two sections are devoted to time and space discretization.

3. Local time integration schemes

In this section we define a whole class of local time integration schemes which comprise LTS and locally implicit methods as special cases. The class has been introduced and analyzed in [7] for second-order ODEs. For the space discretization, we use a *symmetric weighted interior penalty* discontinuous Galerkin method. Details will be given in Section 4. This results in the semidiscrete problem

$$\partial_t^2 u_h = -A_h u_h + f_h, \qquad u_h(0) = u_h^0, \quad \partial_t u_h(0) = v_h^0, \tag{3.1}$$

where A_h, f_h, u_h^0, and v_h^0 denote the spatially discretized operator, source term, and initial values, respectively. The boundary condition (2.1b) is weakly enforced within the operator A_h.

For the spatial mesh $\mathcal{T}_h$ we define a local CFL parameter $\xi_K > 0$ via

$$\xi_K^2 = \kappa|_K h_K^{-2}, \qquad K \in \mathcal{T}_h, \tag{3.2}$$

where h_K denotes the diameter of the element K. Recall that for constant wave speed and a uniform grid, i.e., $\xi_K \equiv \xi$ for all $K \in \mathcal{T}_h$, the leapfrog scheme is stable if $\tau\xi \lesssim 1$. We are interested in the situation, where ξ_K is large on only a few elements elements while it takes small or moderate values on the remaining mesh. To be more precise, we define a disjoint splitting of the mesh into submeshes which lead to a *weak* or *strong* CFL condition, respectively, i.e.,

$$\mathcal{T}_h = \mathcal{T}_{h,w} \,\dot\cup\, \mathcal{T}_{h,s}, \qquad \operatorname{card}(\mathcal{T}_{h,s}) \ll \operatorname{card}(\mathcal{T}_{h,w}), \tag{3.3a}$$

where

$$0 < \xi_K \le \xi_{\max,w} \qquad \text{for all } K \in \mathcal{T}_{h,w}, \tag{3.3b}$$

$$\xi_{\max,w} < \xi_K \le \xi_{\max} \qquad \text{for all } K \in \mathcal{T}_{h,s}. \tag{3.3c}$$

With this notation, the leapfrog scheme on the entire mesh $\mathcal{T}_h$ is stable if $\tau\xi_{\max} \lesssim 1$, and this strong CFL condition must be satisfied even if $\mathcal{T}_h$ only contains a single element. The idea of local time integration methods is to apply the very efficient leapfrog method on as many elements as possible and to modify it on the remaining elements in such a way that stability is guaranteed under a weak CFL condition $\tau\xi_{\max,w} \lesssim 1$. Such schemes are attractive, if $\xi_{\max,w} \ll \xi_{\max}$.

From our previous work on locally implicit methods for Maxwell's equations [36, 37] we know that it is not sufficient to modify the time integration scheme only on the fine elements and thus we decompose the mesh $\mathcal{T}_h$ subject to

$$\mathcal{T}_h = \mathcal{T}_{h,e} \,\dot\cup\, \mathcal{T}_{h,m}, \qquad \mathcal{T}_{h,s} \subset \mathcal{T}_{h,m}, \quad \mathcal{T}_{h,e} \subset \mathcal{T}_{h,w},$$

where $\mathcal{T}_{h,e}$ contains the elements treated with the *explicit* leapfrog scheme and $\mathcal{T}_{h,m}$ contains the elements treated by a *modified* scheme, e.g., an explicit scheme with a weaker CFL condition than the leapfrog method or an implicit scheme. A precise definition of $\mathcal{T}_{h,e}$ and $\mathcal{T}_{h,m}$ is given in Section 4.4 below. To define the local time integration scheme we denote by χ_e and χ_m the indicator functions on $\mathcal{T}_{h,e}$ and $\mathcal{T}_{h,m}$, respectively, i.e., for $v \in L^2(\Omega)$ we define

$$(\chi_b v)|_K = \begin{cases} v|_K, & K \in \mathcal{T}_{h,b}, \\ 0, & K \in \mathcal{T}_h \setminus \mathcal{T}_{h,b}, \end{cases} \qquad b \in \{e, m\}. \tag{3.4}$$

We denote with $\tau > 0$ the time-step size and write $t_n = n\tau$, $n \in \mathbb{N}_0$. To simplify the presentation, we introduce weighted means and second-order differences as

$$\begin{aligned} \langle\!\langle u_h^n \rangle\!\rangle_\theta &= \theta\, u_h^{n+1} + (1-2\theta)\, u_h^n + \theta\, u_h^{n-1}, & \langle\!\langle u_h^n \rangle\!\rangle &= \langle\!\langle u_h^n \rangle\!\rangle_{\frac14}, \\ \langle u_h^n \rangle_\theta &= 2\theta\, u_h^{n+1} + (1-2\theta)\, u_h^n, & \langle u_h^n \rangle &= \langle u_h^n \rangle_{\frac14}, \\ \langle\!\langle u_h^n \rangle\!\rangle &= u_h^{n+1} - 2u_h^n + u_h^{n-1}, \end{aligned}$$

respectively. Here, $\theta \geq 1/4$ is a parameter.

With this notation we define a class of local time integration schemes via an analytic function $\widehat{\Psi} : [0, \infty) \to \mathbb{R}$ satisying $\widehat{\Psi}(0) = 1$ as follows

$$\widehat{\boldsymbol{\Psi}} = \widehat{\Psi}(\tau^2 A_h \chi_m), \tag{3.5a}$$

$$u_h^1 = u_h^0 + \tau\big(I_h - \tfrac14 \tau^2 \widehat{\boldsymbol{\Psi}} A_h\big) v_h^0 + \tfrac12 \tau^2 \widehat{\boldsymbol{\Psi}}\big(-A_h u_h^0 + \widehat{f}_h^0\big), \tag{3.5b}$$

$$u_h^{n+1} - 2u_h^n + u_h^{n-1} = \langle\!\langle u_h^n \rangle\!\rangle = \tau^2 \widehat{\boldsymbol{\Psi}}\big(-A_h u_h^n + \widehat{f}_h^n\big), \tag{3.5c}$$

for $n = 1, 2, \ldots$, where $\widehat{f}_h^n$ denotes a discretization of $f(t_n)$ which is yet to be determined. This class comprises the following special cases:

▷ For

$$\widehat{\Psi}(z) \equiv 1, \qquad \widehat{f}_h^n = f_h^n := f_h(t_n), \tag{3.6}$$

(3.5c) yields the well-known leapfrog recurrence on $\mathcal{T}_h$. In general, (3.5) corresponds to the leapfrog scheme on $\mathcal{T}_{h,e}$, since $\widehat{\Psi}(0) = 1$.

▷ For $\theta \geq 1/4$ and

$$\widehat{\Psi}(z) = \widehat{R}(z) = (1 + \theta z)^{-1}, \qquad \widehat{f}_h^n = \langle\!\langle f_h^n \rangle\!\rangle_\theta, \quad n \geq 1, \qquad \widehat{f}_h^0 = \langle f_h^0 \rangle_\theta, \tag{3.7}$$

the two-step scheme (3.5c) corresponds to a θ-scheme on $\mathcal{T}_{h,m}$ and the leapfrog scheme on $\mathcal{T}_{h,e}$. For $\theta = 1/4$, the scheme (3.5c) is equivalent to the Crank–Nicolson recurrence.

▷ For

$$\widehat{\Psi} = \widehat{P}_p, \qquad \widehat{f}_h^n = f_h^n, \tag{3.8a}$$

the scheme corresponds to the modification [6, eq. (4.1a)] of the LFC scheme [8] on $\mathcal{T}_{h,m}$ and the leapfrog scheme on $\mathcal{T}_{h,e}$. Here, $\widehat{P}_p$ is a polynomial defined as

$$\begin{aligned} \widehat{P}_p(z) z = P_p(z) &= 2 - \frac{2}{T_p(\nu_p^\eta)} T_p\Big(\nu_p^\eta - \frac{z}{\alpha_p}\Big), \\ \alpha_p &= 2\frac{T_p'(\nu_p^\eta)}{T_p(\nu_p^\eta)}, \quad \nu_p^\eta = 1 + \frac{\eta^2}{2p^2}, \end{aligned} \tag{3.8b}$$

where T_p denotes the pth Chebyshev polynomial of first kind ($p \in \mathbb{N}$) and $\eta \geq 0$ is a stabilization parameter. For $f_h \equiv 0$, and a continuous finite element space

discretization with mass lumping, the LTS scheme (3.5c)&(3.8) has been analyzed in [25].

▷ Further alternatives to the implicit θ-scheme or the explicit LFC scheme are exponential integrators, e.g., a Gautschi-type method [33, Chapter XIII]. For a characterization of functions $\widehat{\Psi}$, which allow us to perform the following stability and error analysis, we refer to [6, 7] where the above two-step scheme was proposed and analyzed for (stiff) ODEs.

For the sake of presentation, we focus only on two choices for the modified scheme, namely (3.8), i.e., a LTS method, and (3.7) with $\theta = 1/4$, i.e., a locally implicit scheme comprising leapfrog and Crank–Nicolson methods.

Our main result is the following error bound:

Theorem 3.1. *Let Assumption 2.2 and Assumption 2.3 hold with $\mu \geq 1$. Further, assume that the solution u of (2.1) is sufficiently regular. Consider the local time integration scheme (3.5) complemented with either (3.7) (for $\theta = 1/4$) or (3.8) (for suitable choices of p and η). If $\tau \leq \tau_{\mathrm{CFL}}$, where τ_{CFL} is independent of $\mathcal{T}_{h,s}$ and $\kappa|_{\mathcal{T}_{h,s}}$, then there is a constant $C > 0$ independent of h and τ such that*

$$\|u(t_n) - u_h^n\| \leq C(\tau^2 + h^{k+1}), \qquad t_n \leq T, \tag{3.9}$$

where k denotes the degree of the polynomials of the dG discretization.

In the remaining paper, we will provide more detailed versions of this result and also present their proofs.

4. Spatial discretization

In this section, we introduce the discrete setting and define the discretization with the discontinuous Galerkin method. In addition, we review some properties and estimates on the operator A_h (and its "suboperators" on the submeshes $\mathcal{T}_{h,e}$ and $\mathcal{T}_{h,m}$) required for the error analysis.

4.1. Discrete setting.

With $\mathcal{T}_h$ we denote matching simplicial meshes of Ω, see, e.g., [18, Definition 1.36] for a definition. As usual, the subscript $h = \max_{K\in\mathcal{T}_h} h_K$ refers to the maximal diameter of all mesh elements, where h_K denotes the diameter of a mesh element K. We assume that $\mathcal{T}_h$ matches the partition P_Ω of Ω given in Assumption 2.2, thus, κ is constant on every mesh element $K \in \mathcal{T}_h$. Moreover, we assume that the meshes $\mathcal{T}_h$ are shape-regular, i.e., there exist a constant ρ independent of h such that $h_K/\delta_K \leq \rho$ for all $K \in \mathcal{T}_h$ and all $\mathcal{T}_h$, where δ_K denotes the diameter of the largest ball inscribed in K.

The faces of mesh elements of $\mathcal{T}_h$ are collected in $\mathcal{F}_h = \mathcal{F}_h^{\mathrm{int}} \cup \mathcal{F}_h^{\mathrm{bnd}}$, where the first set collects the interior faces and the second set the boundary faces. For a precise definition of a face $F \in \mathcal{F}_h$ we refer, e.g., to [18, Section 1.2]. The maximum number of mesh faces composing the boundary of a mesh element is denoted by

$$N_\partial = \max_{K\in\mathcal{T}_h} \operatorname{card}\{F \in \mathcal{F}_h \mid F \subset \partial K\},$$

which is in case of matching simplicial meshes given by $N_\partial = d + 1$.

For every interior face $F \in \mathcal{F}_h^{\mathrm{int}}$ we refer to the two neighboring elements sharing this face arbitrarily by $K_{F,1}$ and $K_{F,2}$. We fix this choice and define n_F as the outward unit normal vector pointing from $K_{F,1}$ to $K_{F,2}$. For a boundary face $F \in \mathcal{F}_h^{\mathrm{bnd}}$ the orientation of n_F is always outwards.

Remark 4.1. The restriction to matching simplicial meshes can be dropped. The following results hold true for more general meshes satisfying the shape and contact regularity assumptions [18, Section 1.4.1] as well as an *optimal polynomial approximation* property [18, Section 1.4.4].

As discrete approximation space we use the broken finite element space

$$V_h = \big\{\varphi_h \in L^2(\Omega) \mid \varphi_h|_K \in \mathcal{P}(K) \text{ for all } K \in \mathcal{T}_h\big\},$$

where $\mathbb{P}_d^k(K) \subseteq \mathcal{P}(K) \subset H^{k+1}(K)$ and $\mathbb{P}_d^k$ denotes the set of polynomials of total degree at most k; see, e.g., [23, Chapter 18]. Typically, one chooses $\mathcal{P}(K) = \mathbb{P}_d^k$. We point out that, since our bounds rely on elementwise estimates, it is easy to generalize our analysis to varying polynomial degrees on mesh elements. For the error analysis we also introduce the vector space

$$V_{\star,h} = V_\star + V_h$$

as the sum of $V_\star$ defined in (2.4) and the discrete space V_h.

Further, we define the weighted average of a sufficiently smooth function v over an interior face $F \in \mathcal{F}_h^{\mathrm{int}}$ as

$$\{\!\{v\}\!\}_F^\omega = \frac{\omega_{K_{F,1}}(v|_{K_{F,1}})|_F + \omega_{K_{F,2}}(v|_{K_{F,2}})|_F}{\omega_{K_{F,1}} + \omega_{K_{F,2}}}, \tag{4.1}$$

where $\omega\colon \Omega \to (0,\infty)$ is a given piecewise constant function satisfying $\omega|_K \equiv \omega_K$ for all $K \in \mathcal{T}_h$. Note that, if ω is constant on a face $F \in \mathcal{F}_h^{\mathrm{int}}$, we obtain the usual arithmetic average, i.e., $\{\!\{\cdot\}\!\}_F^\omega = \{\!\{\cdot\}\!\}_F^1$. The jump of v over an interior face $F \in \mathcal{F}_h^{\mathrm{int}}$ is defined as

$$[\![v]\!]_F = (v|_{K_{F,1}})|_F - (v|_{K_{F,2}})|_F.$$

For vector fields these operations act componentwise. On boundary faces $F \in \mathcal{F}_h^{\mathrm{bnd}}$ we set $\{\!\{v\}\!\}_F^\omega = [\![v]\!]_F = v|_F$.

4.2. **Spatially discretized problem.** For the discretization of the operator A we use the *symmetric weighted interior penalty* bilinear form introduced in [22]; see also [18, Chapter 4] and [24, Chapters 38, 41] for more information. The bilinear form $a_h\colon V_{\star,h} \times V_{\star,h} \to \mathbb{R}$ is then given by

$$\begin{aligned} a_h(u_h,\varphi_h) = &\sum_{K\in\mathcal{T}_h} \int_K \kappa\nabla u_h \cdot \nabla\varphi_h \,\mathrm{d}x - \sum_{F\in\mathcal{F}_h} \int_F \{\!\{\kappa\nabla u_h\}\!\}_F^{1/\kappa} \cdot n_F [\![\varphi_h]\!]_F \,\mathrm{d}\sigma \\ &- \sum_{F\in\mathcal{F}_h} \int_F \{\!\{\kappa\nabla \varphi_h\}\!\}_F^{1/\kappa} \cdot n_F [\![u_h]\!]_F \,\mathrm{d}\sigma + \sum_{F\in\mathcal{F}_h} \mathrm{a}_F \int_F [\![u_h]\!]_F [\![\varphi_h]\!]_F \,\mathrm{d}\sigma, \end{aligned} \tag{4.2}$$

where a_F denotes a penalty factor on each face F. The second, third, and fourth terms correspond to jump and flux terms at faces $F \in \mathcal{F}_h$ and are called *consistency*, *symmetry/adjoint consistency*, and *penalty* terms, respectively.

As penalty factor we use $\mathrm{a}_F = \eta_S\, \kappa_F\, h_F^{-1}$ on every face $F \in \mathcal{F}_h$ with a penalty parameter $\eta_S > 0$, the local length scale h_F given by

$$h_F = \begin{cases} \min\{h_{K_{F,1}}, h_{K_{F,2}}\}, & F \in \mathcal{F}_h^{\mathrm{int}}, F = \partial K_{F,1} \cap \partial K_{F,2}, \\ h_K, & F \in \mathcal{F}_h^{\mathrm{bnd}}, F = \partial K \cap \partial\Omega, \end{cases} \tag{4.3}$$

and the material-dependent penalty parameter

$$\kappa_F = \begin{cases} \frac{2\kappa_{K_{F,1}}\kappa_{K_{F,2}}}{\kappa_{K_{F,1}}+\kappa_{K_{F,2}}}, & F \in \mathcal{F}_h^{\text{int}}, F = \partial K_{F,1} \cap \partial K_{F,2}, \\ \kappa_K, & F \in \mathcal{F}_h^{\text{bnd}}, F = \partial K \cap \partial\Omega. \end{cases} \tag{4.4}$$

Note that our choice of the bilinear form a_h coincides with the weighted version in [18, Section 4.5], where a different notation is used.

Remark 4.2. Other choices for the penalty factor a_F and the weight ω are possible; see, e.g., [18, Chapter 4] or [30]. For instance, in $d = 2, 3$ we could have used the local length scale $h_F = \operatorname{diam}(F)$ for every face $F \in \mathcal{F}_h$ as well. For appropriate choices the following results still hold, possibly with minor modifications.

It can be shown that the bilinear form a_h is bounded on $V_{\star,h} \times V_h$ and coercive on V_h with respect to a suitable norm if $\eta_S > \eta_S^* = N_\partial C_{\text{trc}}^2$ see, e.g., [18, Lemma 4.51] or [24, Lemma 41.11]. Here, C_{trc} refers to the constant from the discrete trace inequality (A.3). We emphasize that η_S^* is independent of h_F and the material parameter κ. However, since C_{trc} depends on the shape-regularity constant ρ, the polynomial degree k, and the dimension d, so does η_S^*. For instance, for matching simplicial meshes and $V_h = \mathbb{P}_d^k(\mathcal{T}_h)$ one has $N_\partial = d+1$ and $C_{\text{trc}}^2 \leq (k+1)(k+d)\rho$, hence $\eta_S^* \sim (d+1)(k+1)(k+d)\rho$; see, e.g., [18, Lemma 1.46 and Remark 1.48] and [23, Lemma 12.10].

Assumption 4.3. *The penalty parameter η_S satisfies $\eta_S > N_\partial C_{\text{trc}}^2$.*

With this bilinear form a_h, the spatially discretized problem of the wave equation (2.1) is given by

$$(\partial_t^2 u_h, v_h) = -a_h(u_h, v_h) + (f, v_h) \qquad \text{for all } v_h \in V_h, \tag{4.5a}$$

$$u_h(0) = u_h^0 = \pi_h u^0, \qquad \partial_t u_h(0) = v_h^0 = \pi_h v^0, \tag{4.5b}$$

where we take the L^2-orthogonal projection of the exact values for the initial values; see (4.8) below for a definition. Clearly, other approximations of the initial values could be taken as well, e.g., interpolation. The boundary conditions (2.1b) are weakly enforced through the bilinear form a_h. The error analysis of this semidiscrete problem (with minor modifications in the bilinear form a_h) was carried out in [30].

By introducing the operator $A_h \colon V_{\star,h} \to V_h$, which for $u \in V_{\star,h}$ is defined by

$$(A_h u, \varphi_h) = a_h(u, \varphi_h) \qquad \text{for } \varphi_h \in V_h, \tag{4.6}$$

the semidiscrete scheme (4.5a) can be written in the compact form (3.1). Note that the operator A_h is well-defined by the boundedness of a_h and the Riesz representation theorem. Moreover, by using results from [5] we obtain from the coercivity of the bilinear form a_h (under Assumption 4.3) that there exists a constant $\tilde{c}_{\text{coer}} > 0$, independent of h, such that

$$(A_h u_h, u_h) \geq \tilde{c}_{\text{coer}} \|u_h\|^2 \qquad \text{for all } u_h \in V_h. \tag{4.7}$$

4.3. **Consistency and projections estimates.** Next, we state some properties of A_h as well as projection estimates required for the error analysis. We start with the definitions of the projection operators.

The L^2-orthogonal projection $\pi_h \colon L^2(\Omega) \to V_h$ and the *Ritz/elliptic* projection $\Pi_h \colon V_{\star,h} \to V_h$ are defined such that for $u \in L^2(\Omega)$

$$(\pi_h u, \varphi_h) = (u, \varphi_h) \qquad \text{for all } \varphi_h \in V_h, \tag{4.8}$$

and for $u \in V_{\star,h}$

$$a_h(\Pi_h u, \varphi_h) = a_h(u, \varphi_h) \qquad \text{for all } \varphi_h \in V_h. \tag{4.9}$$

Observe that due to the broken space $V_h \subset L^2(\Omega)$ the L^2-projection works locally on each element, i.e., for $u \in L^2(\Omega)$ we have $\pi_h u|_K = (\pi_h u)|_K$ for all $K \in \mathcal{T}_h$.

Lemma 4.4 (Consistency)**.** *For $u \in V_\star$ we have*

$$A_h \Pi_h u = A_h u = \pi_h A u. \tag{4.10}$$

Proof. We first observe that by $u \in V_\star$ we have $[\![u]\!]_F = 0$ for all $F \in \mathcal{F}_h$ and $[\![\kappa \nabla u]\!]_F = 0$ for all $F \in \mathcal{F}_h^{\text{int}}$. Elementwise integration by parts, cf. [18, Lemma 4.47], then yields

$$\begin{aligned} a_h(u, \varphi_h) &= \sum_{K \in \mathcal{T}_h} \int_K \kappa \nabla u \cdot \nabla \varphi_h \, \mathrm{d}x - \sum_{F \in \mathcal{F}_h} \int_F \{\!\{\kappa \nabla u\}\!\}_F^{1/\kappa} \cdot n_F [\![\varphi_h]\!]_F \, \mathrm{d}\sigma \\ &= - \sum_{K \in \mathcal{T}_h} \int_K \nabla \cdot (\kappa \nabla u) \varphi_h \, \mathrm{d}x = (Au, \varphi_h), \end{aligned}$$

which shows (4.10) by using the corresponding definitions. □

We emphasize that this lemma does not hold true for $u \in H_0^1(\Omega) \cap D(A)$, since $\kappa \nabla u$ admits no trace in L^2 in general. In fact, this is the main reason why we assume $u \in H^{1+\mu}(P_\Omega)$, $\mu > \frac{1}{2}$. For the L^2-projection the following results hold elementwise; see, e.g., [23, Section 18.4].

Lemma 4.5. *For $K \in \mathcal{T}_h$, $F \in \mathcal{F}_h$, $F \subset \partial K$, and $u \in H^{1+\sigma}(\mathcal{T}_h)$, $\sigma > \frac{1}{2}$, there are constants C, depending only on the shape-regularity constant ρ, the polynomial degree k, the dimension d, and the regularity exponent σ, such that*

$$\begin{aligned} &\|u - \pi_h u\|_K \le C h^{r_*+1} |u|_{r_*+1,K}, && \|\nabla u - \nabla \pi_h u\|_K \le C h^{r_*} |u|_{r_*+1,K}, \\ &\|u - \pi_h u\|_F \le C h^{r_*+1/2} |u|_{r_*+1,K}, && \|\nabla u - \nabla \pi_h u\|_F \le C h^{r_*-1/2} |u|_{r_*+1,K}, \end{aligned}$$

where $r_* = \min\{\sigma, k\}$.

For the Ritz projection one obtains with Assumption 2.3 the following optimal estimate.

Lemma 4.6. *Let Assumptions 2.2, 2.3, and 4.3 hold. If $u \in V_\star \cap H^{1+\sigma}(\mathcal{T}_h)$, $\sigma > \frac{1}{2}$, we have*

$$\|u - \Pi_h u\| \le C_R \, |u|_{r_*+1,\mathcal{T}_h} h^r, \qquad r = r_* + \min\{\mu, 1\}, \; r_* = \min\{\sigma, k\},$$

where C_R is independent of h and u.

Proof. By definition (4.9) the Ritz projection Π_h of $u \in V_\star$ is the solution of the elliptic problem: Seek $u_h \in V_h$ such that

$$a_h(u_h, \varphi_h) = \ell(\varphi_h) \qquad \text{for all } \varphi_h \in V_h,$$

where $\ell(\varphi_h) = (Au, \varphi_h)$ (note that by assumption $Au \in L^2(\Omega)$). For a proof of this standard problem we refer to [24, Section 38.3], where the result is shown for $\kappa \equiv 1$ under the regularity $H_0^1(\Omega) \cap H^{1+\sigma}(\Omega)$, $\sigma > \frac{1}{2}$, for the exact solution. The results in there also hold for our regularity assumptions and can be directly extended to the case of $\kappa \not\equiv 1$; see also [24, Chapter 40 and 41] for further information. □

Clearly, if Assumption 2.3 holds with $\mu \geq 1$ and $u \in V_\star \cap H^{k+1}(\mathcal{T}_h)$, we obtain the optimal order h^{k+1} for $V_h = \mathbb{P}_d^k(\mathcal{T}_h)$. Moreover, by definition we always have $\sigma \geq \mu$.

4.4. **Splitting of the mesh.** To complete the construction of the LTS and locally implicit scheme, we have to define the sets $\mathcal{T}_{h,e}$ and $\mathcal{T}_{h,m}$, i.e., the sets of elements treated with the *explicit* leapfrog scheme and the ones treated with the *modified* scheme, respectively.

For this we recall that we are interested in situations where the mesh can be split into two parts $\mathcal{T}_{h,w}$ and $\mathcal{T}_{h,s}$ which require a *weak* and a *strong* CFL condition, respectively and satisfy $\operatorname{card}(\mathcal{T}_{h,s}) \ll \operatorname{card}(\mathcal{T}_{h,w})$; cf. (3.3). In order to avoid that the CFL condition of the leapfrog scheme on $\mathcal{T}_{h,e}$ depends on the strong CFL condition, it is necessary to treat the elements in $\mathcal{T}_{h,s}$ *and* their neighbors with the modified scheme because of the flux terms in the bilinear form a_h; cf. the locally implicit schemes for Maxwell's equations in [36, 37]. More precisely, the decomposition $\mathcal{T}_h = \mathcal{T}_{h,m} \dot\cup \mathcal{T}_{h,e}$ is given by

$$\begin{aligned} \mathcal{T}_{h,m} &= \{K \in \mathcal{T}_h \mid \exists K_s \in \mathcal{T}_{h,s} \ : \ \operatorname{vol}_{d-1}(\partial K \cap \partial K_s) \neq 0\}, \\ \mathcal{T}_{h,e} &= \mathcal{T}_h \setminus \mathcal{T}_{h,m}; \end{aligned} \tag{4.11}$$

cf. [36, Definition 2.3].

For the stability of the local time integration schemes (3.5) it is important to understand the behavior of the operator A_h on the submeshes $\mathcal{T}_{h,e}$ and $\mathcal{T}_{h,m}$. Hence, we define the self-adjoint, positive semidefinite operators

$$A_{h,e} = \chi_e A_h \chi_e, \qquad A_{h,m} = \chi_m A_h \chi_m, \tag{4.12}$$

acting on the submeshes $\mathcal{T}_{h,e}$ and $\mathcal{T}_{h,m}$, respectively. They correspond to the "non-stiff" and "stiff" parts of the semidiscrete differential equation (3.1). By definition of χ_e, χ_m and $\xi_{\max}$, $\xi_{\max,w}$, cf. (3.3), we have

$$4\xi_{\max}^2 \sim \|A_h\|_{V_h} \approx \|A_{h,m}\|_{V_h} \gg \|A_{h,e}\|_{V_h} \sim 4\xi_{\max,w}^2;$$

cf. Lemma A.1 for detailed bounds. Here and in the following, $\|T\|_{V_h} = \|T\|_{V_h \leftarrow V_h}$ denotes the operator norm of an discrete operator $T\colon V_h \to V_h$. In addition, we define a coupling operator $A_{h,em}$ by

$$A_{h,em} = \chi_e A_h \chi_m, \tag{4.13}$$

which acts on the faces between $\mathcal{T}_{h,m}$ and $\mathcal{T}_{h,e}$. By the definition of $\mathcal{T}_{h,e}$ and $\mathcal{T}_{h,m}$ we have $\|A_{h,em}\|_{V_h} \lessapprox \frac{1}{2}\|A_{h,e}\|_{V_h}$; cf. Lemma A.1.

5. Stability and CFL conditions

This section is devoted to the stability analysis of the scheme (3.5). We call the scheme stable if for $f_h \equiv 0$, there is a constant $C = C(u_h^0, v_h^0) > 0$ such that

$$\|u_h^n\| \leq C t_n, \qquad n = 0, 1, 2, \dots. \tag{5.1}$$

5.1. **Representation formula.** Recall that we use the leapfrog method on $\mathcal{T}_{h,e}$ and a modified scheme defined by a suitable function $\widehat{\Psi}$ on $\mathcal{T}_{h,m}$. If the problems on these submeshes decouple, i.e., $A_{h,em} = 0$, then the scheme (3.5) is stable if the following two conditions hold:

(i) the CFL condition of the leapfrog scheme on $\mathcal{T}_{h,e}$ is satisfied, i.e., $\tau^2 \|A_{h,e}\|_{V_h} \leq 4$,

(ii) the scheme defined by $\widehat{\Psi}$ is stable if applied to (3.1) with $A_{h,m}$ instead of A_h.

Unfortunately, this does not hold for LTS methods if $A_{h,em} \neq 0$.

A crucial observation for the stability of the general scheme (3.5) is the fact that the two-step scheme (3.5c) is equivalent to the leapfrog scheme applied to the modified equation

$$\partial_t^2 u_h(t) = -A_h^\Psi u_h(t) + \widehat{\boldsymbol{\Psi}} f_h(t) \tag{5.2a}$$

with self-adjoint operator

$$A_h^\Psi = \widehat{\boldsymbol{\Psi}} A_h = \widehat{\Psi}(\tau^2 A_h \chi_m) A_h. \tag{5.2b}$$

Moreover, we have the following representation formula.

Lemma 5.1. *The approximations u_h^n of the two-step scheme (3.5c) satisfy*

$$u_h^n = \boldsymbol{\mathcal{C}}_n^\Psi u_h^0 + \boldsymbol{\mathcal{S}}_n^\Psi \big(u_h^1 - \boldsymbol{\mathcal{C}}_1^\Psi u_h^0\big) + \sum\nolimits_{j=1}^{n-1} \boldsymbol{\mathcal{S}}_{n-j}^\Psi \widehat{\boldsymbol{\Psi}} \widehat{f}_h^j, \qquad n \geq 0, \tag{5.3a}$$

with operators $\boldsymbol{\mathcal{C}}_n^\Psi$, $\boldsymbol{\mathcal{S}}_n^\Psi \colon V_h \to V_h$ defined by

$$\boldsymbol{\mathcal{C}}_n^\Psi = T_n(X_h), \qquad \boldsymbol{\mathcal{S}}_n^\Psi = U_{n-1}(X_h), \qquad X_h = I_h - \tfrac{1}{2}\tau^2 A_h^\Psi, \tag{5.3b}$$

where T_n and U_n denote the nth Chebyshev polynomials of first and second kind, respectively (with $U_{-1} \equiv 0$).

Proof. We modify the proof of [8, Theorem 3.3] since it requires that the CFL condition (5.5) holds. First, we define generating functions as formal power series

$$\mathbf{u}(\zeta) = \sum_{n=0}^\infty u_h^n \zeta^n, \qquad \widehat{\mathbf{f}}(\zeta) = \sum_{n=0}^\infty \widehat{f}_h^n \zeta^n.$$

Next, we multiply the recursion (3.5c) by ζ^{n+1} and sum over $n \geq 1$. This yields

$$\boldsymbol{\varrho}(\zeta)\mathbf{u}(\zeta) = u_h^0 + \zeta u_h^1 - 2\zeta X_h u_h^0 + \tau^2 \zeta \big(\widehat{\mathbf{f}}(\zeta) - \widehat{f}_h^0\big), \tag{5.4a}$$

$$\boldsymbol{\varrho}(\zeta) = \zeta^2 I_h - 2\zeta X_h + I_h. \tag{5.4b}$$

To prove the representation formula, we first observe that X_h is a self-adjoint operator, which only has real eigenvalues. By [1, Ch. 22] we have

$$\boldsymbol{\varrho}(\zeta)^{-1} = \sum_{n=0}^\infty U_n(X_h)\zeta^n = \sum_{n=0}^\infty \boldsymbol{\mathcal{S}}_{n+1}^\Psi \zeta^n.$$

Comparing the coefficients of ζ^n in (5.4a) yields

$$u_h^n = \boldsymbol{\mathcal{S}}_{n+1}^\Psi u_h^0 + \boldsymbol{\mathcal{S}}_n^\Psi \Big(u_h^1 - 2X_h\, u_h^0\Big) + \tau^2 \sum_{\ell=1}^{n-1} \boldsymbol{\mathcal{S}}_{n-\ell}^\Psi \widehat{f}_h^\ell.$$

The identity $\boldsymbol{\mathcal{C}}_n^\Psi = \boldsymbol{\mathcal{S}}_{n+1}^\Psi - \boldsymbol{\mathcal{S}}_n^\Psi X_h$ completes the proof. □

Thus, stability is guaranteed by the well-known CFL condition of the leapfrog scheme, namely for

$$\tau \leq \tau_{\mathrm{CFL}} \coloneqq \max\{\tau > 0 \text{ s.t. all eigenvalues } \lambda \text{ of } \tau^2 A_h^\Psi \text{ satisfy } \lambda \in [0,4]\}. \tag{5.5}$$

Note that we have $\tau_{\mathrm{CFL}} > 0$ because of $\widehat{\Psi}(0) = 1$. Moreover, (5.5) is sharp, meaning that if the self-adjoint operator $\tau^2 A_h^\Psi$ has an eigenvalue outside of $[0,4]$, then $\|u_h^n\|$ grows exponentially in n. This can be seen directly from (5.3) by choosing the initial values u_h^0 and v_h^0 as a corresponding eigenfunction.

Unfortunately, (5.5) is not of practical use, because τ_{CFL} cannot be computed explicitly for a given space discretization in general. Thus, we next show sufficient conditions in terms of the operators $A_{h,m}$, $A_{h,e}$, and $A_{h,em}$ and the function $\widehat{\Psi}$.

5.2. **CFL conditions.** Since we use an explicit scheme on $\mathcal{T}_{h,e}$, stability is subject to a CFL condition. In this section, we present explicit conditions for local time integration methods, starting with the LTS scheme (3.5)&(3.8).

Lemma 5.2. *Let $\vartheta \in (0,1]$. Then the LTS scheme (3.5)&(3.8) is stable for all $\tau > 0$ satisfying*

$$\tau^2 \le \tau_{\mathrm{LTS}}(\vartheta)^2 = \max\Big\{ \frac{4\vartheta^2}{\|A_h\|_{V_h}}, \min\Big\{ \frac{\beta_p^2}{\|A_{h,m}\|_{V_h}}, \frac{4\gamma\vartheta^2}{\|A_{h,e}\|_{V_h}} \Big\} \Big\} \tag{5.6a}$$

with $\varrho = \|A_{h,em}\|_{V_h}/\|A_{h,e}\|_{V_h}$ and

$$\beta_p^2 = \alpha_p(\nu_p^\eta + 1), \quad \gamma = \frac{2}{1 + (1 + 4\varrho^2 m_1^{-1})^{1/2}}, \quad m_1 = \frac{1}{2}\Big(1 - \frac{1}{T_p(\nu_p^\eta)}\Big). \tag{5.6b}$$

Proof. The statement directly follows from Theorem 3.14 (with $\mathbf{g} = 0$) together with Lemmas 3.17, 5.4, and 5.5 in [7]. □

Observe that the CFL condition (5.6a) is never stronger than that of the leapfrog scheme applied on the entire mesh $\mathcal{T}_h$. A detailed discussion on the CFL condition and the choice of the parameters p and ν_p^η can be found in [7, Sections 3.2, 3.4, 5.1, and 5.4]. In particular, $\nu_p^\eta = 1 + \eta^2/(2p^2)$ in (3.8a) implies that m_1 and $\beta_p^2/(4p^2)$ can be bounded in terms of η but independent of the polynomial degree p; see [7, Lemma 5.5] and [6, Lemma A.7]. Extensive numerical observations showed that $\eta = 1/2$ (in which case we have $\beta_p^2/(4p^2) \ge 0.9162$) is sufficient for stability and in many cases, even $\eta = 0.1$ worked well (which gives $\beta_p^2/(4p^2) \ge 0.9963$). A comparison to the CFL condition given in [25] can be found in [7, Remark 5.6]

Note also that there is a direct relation between $\tau_{\mathrm{LTS}}(\vartheta)$ and the CFL parameters introduced in (3.3b), namely

$$\tau_{\mathrm{LTS}}(\vartheta)^2 \sim \max\Big\{ \frac{1}{\xi_{\max}^2}, \min\Big\{ \frac{\beta_p^2}{4\xi_{\max}^2}, \frac{\gamma\vartheta^2}{\xi_{\max,w}^2} \Big\} \Big\}.$$

The polynomial degree p should be selected such that

$$\frac{\gamma\vartheta^2}{\xi_{\max,w}^2} \approx \frac{\beta_p^2}{4\xi_{\max}^2} \lesssim \frac{p^2}{\xi_{\max}^2}.$$

Hence, as a rule of thumb, we recommend to choose $p \gtrsim \xi_{\max}/\xi_{\max,w}$. Then, the CFL condition is independent of ξ_K for $K \in \mathcal{T}_{h,s}$.

The situation for the locally implicit scheme is much simpler. For a proof of the following lemma we refer again to [6, 7].

Lemma 5.3. *Let $\vartheta \in (0,1]$ and $\theta \ge \frac{1}{4}$. Then the locally implicit scheme (3.5)&(3.7) is stable for all $\tau > 0$ satisfying*

$$\tau^2 \le \tau_{\mathrm{LI}}(\vartheta)^2 := \frac{4\vartheta^2}{\|A_{h,e}\|_{V_h}}. \tag{5.7}$$

The lemma states that the CFL condition of the locally implicit scheme coincides with the one for the leapfrog scheme applied to the semidiscrete problem (3.1) on

$\mathcal{T}_{h,e}$. Hence, it is completely independent of the parameters on the mesh $\mathcal{T}_{h,s}$ and of the coupling operator $A_{h,em}$. In particular, we have

$$\tau_{\mathrm{LI}}(\vartheta)^2 = \frac{4\vartheta^2}{\|A_{h,e}\|_{V_h}} \sim \frac{\vartheta^2}{\xi^2_{\max,w}}.$$

Under the above CFL conditions we further have the following stability estimates; see [7] and [6, Section 5.3 and 5.5].

Lemma 5.4. *Let $\vartheta \in (0,1)$ and $n \in \mathbb{N}$.*

(a) For $\tau \le \tau_{\mathrm{CFL}}$ we have

$$\|\boldsymbol{\mathcal{C}}_n^{\Psi}\|_{V_h} \le 1, \quad \tau\|\boldsymbol{\mathcal{S}}_n^{\Psi}\|_{V_h} \le t_n. \tag{5.8}$$

(b) If $\tau \le \tau_{\mathrm{LTS}}(\vartheta)$ and $\widehat{\Psi} = \widehat{P}_p$ defined in (3.8a), then there is a constant $c_{\mathrm{LTS}} = c_{\mathrm{LTS}}(\eta, \tilde{c}_{\mathrm{coer}}^{-1}) > 0$ such that

$$\tau\,\|\boldsymbol{\mathcal{S}}_n^{\Psi}\|_{V_h} \le c_{\mathrm{LTS}}^{\vartheta} := c_{\mathrm{LTS}}(1-\vartheta^2)^{-1/2}. \tag{5.9}$$

(c) If $\tau \le \tau_{\mathrm{LI}}(\vartheta)$ and $\widehat{\Psi}$ defined in (3.7) with $\theta = \frac{1}{4}$, then

$$\tau\,\|\boldsymbol{\mathcal{S}}_n^{\Psi}\widehat{\boldsymbol{\Psi}}\|_{V_h} \le c_{\mathrm{LI}}^{\vartheta} := \tilde{c}_{\mathrm{coer}}^{-1}(1-\vartheta^2)^{-1/2}. \tag{5.10}$$

Here, $\tilde{c}_{\mathrm{coer}}$ is defined in (4.7). For $\vartheta = 1$ we formally set $c_{\mathrm{LTS}}^{\vartheta}, c_{\mathrm{LI}}^{\vartheta} = \infty$.

5.3. **Conservation of a perturbed energy.** We conclude this section by showing that the two-step scheme (3.5c) of the local time integrator conserves a perturbed energy. Recall that, if $f \equiv 0$,

$$\mathcal{E}(u) = \tfrac{1}{2}\|\partial_t u\|^2 + \tfrac{1}{2}(Au,u) \qquad \text{and} \qquad \mathcal{E}_h(u_h) = \tfrac{1}{2}\|\partial_t u_h\|^2 + \tfrac{1}{2}(A_h u_h, u_h)$$

are conserved quantities for (2.1) and (3.1), respectively.

Lemma 5.5. *For $f \equiv 0$, the perturbed energy of the local time integrator (3.5c)*

$$\mathcal{E}_{h,\tau}^n = \big\|\tfrac{1}{2\tau}(u_h^{n+1} - u_h^{n-1})\big\|^2 + (A_h^{\Psi}u_h^n, u_h^n) - \tfrac{1}{4}\tau^2\|A_h^{\Psi}u_h^n\|^2, \qquad n \in \mathbb{N},$$

is conserved, i.e., $\mathcal{E}_{h,\tau}^n = \mathcal{E}_{h,\tau}^1$ for all $n \ge 1$.

Proof. By taking the sum and difference of two consecutive steps of the two-step scheme (3.5c) we obtain

$$\begin{aligned}\|u_h^{n+2} - u_h^n\|^2 - \|u_h^{n+1} - u_h^{n-1}\|^2 &= \big(-\tau^2 A_h^{\Psi}(u_h^{n+1} + u_h^n), \big(4I_h - \tau^2 A_h^{\Psi}\big)(u_h^{n+1} - u_h^n)\big) \\ &= -4\tau^2\big(A_h^{\Psi}u_h^{n+1}, u_h^{n+1}\big) + 4\tau^2\big(A_h^{\Psi}u_h^n, u_h^n\big) + \tau^4\|A_h^{\Psi}u_h^{n+1}\|^2 - \tau^4\|A_h^{\Psi}u_h^n\|^2.\end{aligned}$$

Rearranging this formula and dividing by $4\tau^2$ yields $\mathcal{E}_{h,\tau}^{n+1} = \mathcal{E}_{h,\tau}^n$, which shows the claim. □

We point out that by a suitable adaption of the first term in $\mathcal{E}_{h,\tau}^n$ for $n = 0$ one also can show $\mathcal{E}_{h,\tau}^1 = \mathcal{E}_{h,\tau}^0$; see [6, Section 3.3.2] for related computations. Moreover, by using the self-adjointness of A_h^{Ψ} a simple calculation shows that $\mathcal{E}_{h,\tau}^n$ is nonnegative for all $n \in \mathbb{N}$ under the abstract CFL condition (5.5).

6. Error analysis

After recalling the stability results in the last section, we now turn towards the error analysis. For a more compact notation we abbreviate

$$\widetilde{u}^n = u(t_n), \qquad f^n = f(t_n), \qquad f_h^n = \pi_h f^n.$$

To bound the fully discrete error $e^n = \widetilde{u}^n - u_h^n$ between the exact solution $u(t_n)$ and the approximations u_h^n, we split it into a projection error e_π^n and a discrete error e_h^n which stems from the time discretization of the spatially discretized equation, i.e.,

$$e^n = \widetilde{u}^n - u_h^n = e_\pi^n + e_h^n, \qquad e_\pi^n = \widetilde{u}^n - \Pi_h \widetilde{u}^n, \quad e_h^n = \Pi_h \widetilde{u}^n - u_h^n \in V_h.$$

Since the projection error e_π^n is bounded by Lemma 4.6, we focus on the discrete error.

To derive an error bound for e_h^n, we insert the Ritz projected solution $\Pi_h \widetilde{u}^n$ into the general scheme (3.5c) to define a defect d_h^n via

$$\Pi_h \mathbb{(}\widetilde{u}^n\mathbb{)} = \tau^2 \widehat{\mathbf{\Psi}}(-A_h \Pi_h \widetilde{u}^n + \widehat{f}_h^n) + d_h^n, \qquad n = 1, 2, \dots . \tag{6.1}$$

Subtracting (3.5) from (6.1) shows the error recursion

$$\mathbb{(}e_h^n\mathbb{)} = -\tau^2 \widehat{\mathbf{\Psi}} A_h e_h^n + d_h^n, \qquad n = 1, 2, \dots,$$

which leads with Lemma 5.1 to a representation formula for the discrete error

$$e_h^n = \boldsymbol{\mathcal{C}}_n^\Psi e_h^0 + \boldsymbol{\mathcal{S}}_n^\Psi \big(e_h^1 - \boldsymbol{\mathcal{C}}_1^\Psi e_h^0\big) + \sum\nolimits_{j=1}^{n-1} \boldsymbol{\mathcal{S}}_{n-j}^\Psi d_h^j. \tag{6.2}$$

For the error e_h^1 of the first step, we replace u_h^1, u_h^0 in (3.5b) by $\Pi_h \widetilde{u}^1$, $\Pi_h \widetilde{u}^0$, respectively, yielding

$$\Pi_h \widetilde{u}^1 = \Pi_h \widetilde{u}^0 + \tau \big(I_h - \tfrac{1}{4}\tau^2 A_h^\Psi\big) v_h^0 + \tfrac{1}{2}\tau^2 \widehat{\mathbf{\Psi}}(-A_h \Pi_h \widetilde{u}^0 + \widehat{f}_h^0) + d_h^0 \tag{6.3}$$

with a defect d_h^0 which is again to be determined (note that we leave v_h^0 unchanged). Subtracting (3.5b) from this equation, inserting this into the representation formula (6.2), and using $I_h - \frac{1}{2}\tau^2 A_h^\Psi = \boldsymbol{\mathcal{C}}_1^\Psi$ leads to

$$e_h^n = \boldsymbol{\mathcal{C}}_n^\Psi e_h^0 + \boldsymbol{\mathcal{S}}_n^\Psi d_h^0 + \sum\nolimits_{j=1}^{n-1} \boldsymbol{\mathcal{S}}_{n-j}^\Psi d_h^j. \tag{6.4}$$

For the next steps in the error analysis, in particular for the derivation of the defects, we distinguish between the LTS scheme and the locally implicit scheme. A crucial step for the error analysis of both schemes consists in the application of the following identity which, roughly speaking, allows us to express two discrete spatial derivatives (via the operator A_h^Ψ) by a second-order central difference quotient.

Lemma 6.1. *Let $\widetilde{\Delta}_*^k \in V_h$, $k = 0, 1, \dots, n$. Then $\Delta_*^k = -\tau^2 A_h^\Psi \widetilde{\Delta}_*^k$ satisfies*

$$\tfrac{1}{2}\boldsymbol{\mathcal{S}}_n^\Psi \Delta_*^0 + \sum_{j=1}^{n-1} \boldsymbol{\mathcal{S}}_{n-j}^\Psi \Delta_*^j = \boldsymbol{\mathcal{C}}_n^\Psi \widetilde{\Delta}_*^0 - \widetilde{\Delta}_*^n + \boldsymbol{\mathcal{S}}_n^\Psi (\widetilde{\Delta}_*^1 - \widetilde{\Delta}_*^0) + \sum_{j=1}^{n-1} \boldsymbol{\mathcal{S}}_{n-j}^\Psi \mathbb{(}\widetilde{\Delta}_*^j\mathbb{)}. \tag{6.5}$$

Proof. We refer to [7, Lemma 4.3] and [6, Lemma 5.22], where the same result is shown for matrices instead of discrete operators and a special choice of $\widetilde{\Delta}_*^n$. □

6.1. **Explicit LTS scheme.** We start with the LTS scheme (3.5)&(3.8), i.e., we have $\widehat{\mathbf{\Psi}} = \widehat{P}_p(\tau^2 A_h \chi_m)$ and $\widehat{f}_h^n = f_h^n$ in (6.1) and (6.3). The main idea is to consider the defects d_h^n as perturbations of the defects of the leapfrog scheme. Since we rely on Taylor expansion for the defects of the time discretization, we abbreviate with

$$\delta_{k,j,\pm}^n = \int_{t_n}^{t_{n\pm1}} \kappa_{n,\pm}^{(k-1)}(s)\, \partial_t^{j+k} u(s)\, \mathrm{d}s, \qquad \kappa_{n,\pm}^{(k)}(s) = \frac{1}{k!}(t_{n\pm1} - s)^k, \tag{6.6}$$

the remainder terms of the $(k-1)$st-order Taylor polynomial of $\partial_t^j \widetilde{u}^{n\pm1}$ at t_n.

Lemma 6.2. *Let u be the solution of (2.1). If $u \in C(0,T;V_\star) \cap W^{4,1}(0,T;L^2(\Omega))$, then the defect d_h^n of the LTS scheme (3.5c)&(3.8) defined in (6.1) satisfies*

$$d_h^n = d_{\mathrm{LF}}^n + \Delta_{\mathrm{E}}^n, \quad \Delta_{\mathrm{E}}^n = \tau^2 (I_h - \widehat{\mathbf{\Psi}}) \pi_h \partial_t^2 \widetilde{u}^n, \qquad n = 1, 2, \dots, \tag{6.7a}$$

where

$$d_{\mathrm{LF}}^n = (\Pi_h - \pi_h)(\!|\widetilde{u}^n|\!) + \pi_h \delta_{\mathrm{LF}}^n, \quad \delta_{\mathrm{LF}}^n = \delta_{4,0,+}^n + \delta_{4,0,-}^n, \tag{6.7b}$$

denotes the defect of the leapfrog scheme.

Proof. From (6.1) we obtain

$$d_h^n - \Pi_h(\!|\widetilde{u}^n|\!) = -\tau^2 \widehat{\mathbf{\Psi}} \big(\pi_h (-A \widetilde{u}^n + f^n) \big) = -\tau^2 \widehat{\mathbf{\Psi}} \pi_h \partial_t^2 u(t_n),$$

where we used the consistency (4.10) of A_h, which follows from the assumption that $\widetilde{u}^n \in V_\star$, as well as (2.3). By Taylor expansion we further have that

$$(\!|\widetilde{u}^n|\!) = \tau^2 \partial_t^2 \widetilde{u}^n + \delta_{\mathrm{LF}}^n. \tag{6.8}$$

Taking the $L^2(\Omega)$-projection of this identity and inserting it into the above equation proves (6.7). □

For the defect d_h^0 of the first time step we have the following.

Lemma 6.3. *Let u be the solution of (2.1). If $u \in C^1(0,T;V_\star) \cap W^{3,1}(0,T;L^2(\Omega))$, then the defect d_h^0 of the starting value of the LTS scheme (3.5b)&(3.8) defined in (6.3) satisfies*

$$d_h^0 = d_{\mathrm{LF}}^0 + \tfrac{1}{4}\tau^3 A_h^\Psi \pi_h \partial_t \widetilde{u}^0 + \tfrac{1}{2}\Delta_{\mathrm{E}}^0, \qquad d_{\mathrm{LF}}^0 = (\Pi_h - \pi_h)\big(\widetilde{u}^1 - \widetilde{u}^0\big) + \pi_h \delta_{3,0,+}^0, \tag{6.9}$$

with Δ_{E}^0 defined as in Lemma 6.2.

Proof. The representation of the defect follows from (6.3) by using again (4.10), $v_h^0 = \pi_h \partial_t \widetilde{u}^0$, and Taylor expansion. □

With these two lemmas we are in the position to prove the error result for the LTS scheme (3.5)&(3.8). The problematic terms for an error estimate are the defects Δ_{E}^n. To see this, we first observe that because of $\widehat{P}_p(0) = 1$ there exists a polynomial $\widetilde{P}_p \colon \mathbb{R} \to \mathbb{R}$ with

$$\widehat{P}_p(z) = 1 + \widetilde{P}_p(z) z. \tag{6.10}$$

A naive estimate would then lead to

$$\begin{aligned} \|\Delta_{\mathrm{E}}^n\| &\le \tau^2 \|(I_h - \widehat{\mathbf{\Psi}})(\pi_h - I_h)\partial_t^2 \widetilde{u}^n\| + \tau^4 \|\widetilde{\Psi}(\tau^2 A_h \chi_m) A_h \chi_m \partial_t^2 \widetilde{u}^n\| \\ &\le C\tau^2 \big(h^{r_*+1} |\partial_t^2 \widetilde{u}^n|_{r_*+1,\mathcal{T}_h} + \tau^2 \|A_h \chi_m \partial_t^2 \widetilde{u}^n\| \big), \end{aligned}$$

where we additionally used the boundedness of $I_h - \widehat{\mathbf{\Psi}}$ and $\widetilde{\Psi}(\tau^2 A_h \chi_m)$ under the CFL condition (5.6) (see [7]) as well as Lemma 4.6. However, the second term cannot be bounded uniformly in h in general; see Lemma A.2 below. Thus, such an estimate would yield suboptimal convergence rates. A similar behavior occurs for locally implicit schemes for Maxwell's equations; see, e.g., [36]. The remedy consists in using the identity (6.5) in Lemma 6.1.

Theorem 6.4. *Let $\sigma > \frac{1}{2}$, $\vartheta \in (0,1]$, $\tau \le \tau_{\mathrm{LTS}}(\vartheta)$ defined in (5.6), and let Assumptions 2.2, 2.3, and 4.3 hold. Further, assume that the solution u of (2.1) satisfies*

$$u \in C^2(0,T; V_\star \cap H^{1+\sigma}(\mathcal{T}_h)) \cap W^{4,1}(0,T; L^2(\Omega)). \tag{6.11}$$

Then, for $t_n \le T$, the approximations u_h^n of the LTS scheme (3.5)&(3.8) satisfy

$$\|u(t_n) - u_h^n\| \le C \min\{c_{\mathrm{LTS}}^{\vartheta}, t_n\}(\tau^2 + h^r), \qquad r = \min\{\sigma, k\} + \min\{\mu, 1\}, \tag{6.12}$$

where C only depends on C_R, η defined in (3.8b), and u and its derivatives.

Proof. We first notice that $\widehat{\Psi}(\tau^2 A_{h,m})$ is invertible for $\tau \le \tau_{\mathrm{LTS}}(1)$; see [7, Section 3]. Together with the definition of the polynomial $\widetilde{P}_p$ in (6.10) we then have for the defect Δ_{E}^n given in (6.7a)

$$\Delta_{\mathrm{E}}^n = -\tau^4 \widetilde{\Psi}(\tau^2 A_h \chi_m) A_h \chi_m \, \pi_h \partial_t^2 \widetilde{u}^n = -\tau^2 A_h^{\Psi} \widetilde{\Delta}_{\mathrm{E}}^n, \tag{6.13a}$$

with

$$\widetilde{\Delta}_{\mathrm{E}}^n = \tau^2 \chi_m \, \widehat{\Psi}(\tau^2 A_{h,m})^{-1} \widetilde{\Psi}(\tau^2 A_{h,m}) \chi_m \, \pi_h \partial_t^2 \widetilde{u}^n. \tag{6.13b}$$

Hence, employing (6.4), (6.7), (6.9), as well as Lemma 6.1 with $\Delta_*^n = \Delta_{\mathrm{E}}^n$, taking the norm, and using the stability estimates in (5.8), (5.9) yields

$$\begin{aligned}\|e_h^n\| \le \|e_h^0\| &+ \min\{c_{\mathrm{LTS}}^{\vartheta}, t_n\} \tfrac{1}{\tau} \Big(\|d_{\mathrm{LF}}^0\| + \sum\nolimits_{j=1}^{n-1} \|d_{\mathrm{LF}}^j\| + \tfrac{1}{4}\tau^3 \|A_h^{\Psi} \pi_h \partial_t \widetilde{u}^0\| \Big) \\ &+ \|\widetilde{\Delta}_{\mathrm{E}}^n\| + \|\widetilde{\Delta}_{\mathrm{E}}^0\| + \min\{c_{\mathrm{LTS}}^{\vartheta}, t_n\} \tfrac{1}{\tau} \Big(\|\widetilde{\Delta}_{\mathrm{E}}^1 - \widetilde{\Delta}_{\mathrm{E}}^0\| + \sum\nolimits_{j=1}^{n-1} \|(\!|\widetilde{\Delta}_{\mathrm{E}}^j|\!)\| \Big).\end{aligned}$$

The terms are bounded separately. For e_h^0 we have by the definition of π_h and Lemma 4.6

$$\|e_h^0\| = \|\pi_h(\Pi_h \widetilde{u}^0 - \widetilde{u}^0)\| \le \|\Pi_h \widetilde{u}^0 - \widetilde{u}^0\| \le C_R |u^0|_{r_*+1, \mathcal{T}_h} \, h^r.$$

For the leapfrog defects defined in (6.7b) and (6.9) we have by Taylor expansion, the definition of $\delta_{k,j,\pm}^n$ in (6.6), and again Lemma 4.6

$$\begin{aligned}\tfrac{1}{\tau}\Big(\|d_{\mathrm{LF}}^0\| + \sum\nolimits_{j=1}^{n-1} \|d_{\mathrm{LF}}^j\| \Big) &\le C_R \max_{s\in[0,\tau]} |\partial_t u(s)|_{r_*+1,\mathcal{T}_h} \, h^r + \tfrac{1}{6} \max_{s\in[0,\tau]} \|\partial_t^3 u(s)\| \, \tau^2 \\ &\quad + C_R \int_0^{t_n} |\partial_t^2 u(s)|_{r_*+1,\mathcal{T}_h} \, \mathrm{d}s \, h^r + \tfrac{1}{3} \int_0^{t_n} \|\partial_t^4 u(s)\| \, \mathrm{d}s \, \tau^2.\end{aligned}$$

Moreover, since $\tau^2 \|A_h^{\Psi}\| \le 4$ and $\|\widehat{\mathbf{\Psi}}\| \le c_{\widehat{\mathbf{\Psi}}}$ under the CFL condition $\tau \le \tau_{\mathrm{LTS}}(1)$ (see again [7, Section 3]), we have with Lemma 4.5

$$\begin{aligned}\tfrac{1}{4}\tau^2 \|A_h^{\Psi} \pi_h \partial_t \widetilde{u}^0\| &\le \|\pi_h \partial_t \widetilde{u}^0 - \partial_t \widetilde{u}^0\| + \tfrac{1}{4} \|\widehat{\mathbf{\Psi}} A_h \partial_t \widetilde{u}^0\| \, \tau^2 \\ &\le C |\partial_t u^0|_{r_*+1,\mathcal{T}_h} \, h^{r_*+1} + \tfrac{1}{4} c_{\widehat{\mathbf{\Psi}}} \|A \partial_t \widetilde{u}^0\| \, \tau^2.\end{aligned}$$

For the terms involving $\widetilde{\Delta}_{\mathrm{E}}^j$ we observe that under the CFL condition $\tau \leq \tau_{\mathrm{LTS}}(\vartheta)$ we have with [7, Lemma 3.2] for $u \in L^2(\Omega)$

$$\|\chi_m \widehat{\Psi}(\tau^2 \chi_m A_h \chi_m)^{-1} \widetilde{\Psi}(\tau^2 \chi_m A_h \chi_m)\chi_m \pi_h u\| \leq \widetilde{m}_3 \|\chi_m \pi_h u\| \leq \widetilde{m}_3 \|\chi_m u\|,$$

since π_h and χ_m commute by definition. Note that the constant $\widetilde{m}_3 = \widetilde{m}_3(\eta)$ can be bounded independent of the degree p of the LFC polynomial (3.8b); see [7, Section 5.1]. Hence, we obtain $\|\widetilde{\Delta}_{\mathrm{E}}^n\| \leq \widetilde{m}_3 \|\chi_m \partial_t^2 \widetilde{u}^n\|$ and $\|\widetilde{\Delta}_{\mathrm{E}}^0\| \leq \widetilde{m}_3 \|\chi_m \partial_t^2 \widetilde{u}^0\|$. Moreover, again with Taylor expansion, we have

$$\tfrac{1}{\tau}\Big(\|\widetilde{\Delta}_{\mathrm{E}}^1 - \widetilde{\Delta}_{\mathrm{E}}^0\| + \sum\nolimits_{j=1}^{n-1} \|(\!|\widetilde{\Delta}_{\mathrm{E}}^j|\!)\|\Big) \leq \widetilde{m}_3 \bigg(\max_{s\in[0,\tau]} \|\chi_m \partial_t^3 u(s)\| + 2\int_0^{t_n} \|\chi_m \partial_t^4 u(s)\| \,\mathrm{d}s\bigg)\tau^2.$$

Collecting these bounds and inserting them into the first estimate yields the bound for $\|e_h^n\|$. The triangle inequality and Lemma 4.6 complete the proof. □

Remark 6.5. The regularity assumptions (6.11) we pose for the exact solution u of (2.1) coincides with those imposed for the leapfrog or θ-schemes in [32, 39] to prove (optimal) error bounds in the $L^2(\Omega)$-norm. In contrast, the error analysis for the LTS scheme in [25, Theorem 3.11] requires $u \in W^{8,\infty}(0,T;H^{k+1}(\Omega))$ for the exact solution. Moreover, compared to the error bounds in [32, 39] our result holds without an additional factor of t_n for $\vartheta < 1$, since $\min\{c_{\mathrm{LTS}}^{\vartheta}, t_n\} \leq c_{\mathrm{LTS}}^{\vartheta}$.

6.2. **Locally implicit scheme.** Next, we turn towards the error bound for the locally implicit scheme (3.5)&(3.7) with $\theta = \frac{1}{4}$, i.e., we have $\widehat{\boldsymbol{\Psi}} = \widehat{R}(\tau^2 A_h \chi_m)$ and $\widehat{f}_h^n = \langle\!\langle f_h^n \rangle\!\rangle$ for $n \geq 1$, as well as $\widehat{f}_h^0 = \langle f_h^0 \rangle$ in (6.1) and (6.3).

In principle, we could use the defect from the LTS schemes in Lemma 6.2 by additionally taking the modification of $\widehat{f}_h^n$ into account, i.e.,

$$d_h^n = d_{\mathrm{LF}}^n + \Delta_{\mathrm{E}}^n - \tfrac{1}{4}\tau^2 \widehat{\boldsymbol{\Psi}}(f_h^{n+1} - 2f_h^n + f_h^{n-1})$$

with Δ_{E}^n and d_{LF}^n defined in (6.7). By assuming $f \in C^2(0,T;L^2(\Omega))$ we could then perform the analysis analogously. However, since for $\theta = \frac{1}{4}$ the locally implicit scheme does not admit a uniform bound for $\tau\|\boldsymbol{\mathcal{S}}_n^{\Psi}\|$ like (5.9) for the LTS scheme, the error bound (6.12) would hold with t_n instead of $\min\{c(\vartheta), t_n\}$ for a constant $c(\vartheta) > 0$.

As remedy to this problem we want to employ the bound (5.10). To do so, we consider the defects as perturbation of the defects of the implicit trapezoidal rule or θ-schemes instead of the ones of the leapfrog scheme.

Lemma 6.6. *Let u be the solution of (2.1). If $u \in C^1(0,T;V_\star) \cap W^{4,1}(0,T;L^2(\Omega))$, then the defect d_h^n of the locally implicit scheme (3.5c)&(3.7) defined in (6.1) satisfies*

$$\text{(6.14a)}\quad d_h^n = \widehat{\boldsymbol{\Psi}} d_\theta^n - \tfrac{1}{4}\tau^2 \widehat{\boldsymbol{\Psi}} A_h \chi_e d_{\mathrm{LF}}^n + \Delta_{\mathrm{I}}^n, \qquad \Delta_{\mathrm{I}}^n = -\tfrac{1}{4}\tau^4 \widehat{\boldsymbol{\Psi}} A_h \chi_e \pi_h \partial_t^2 \widetilde{u}^n,$$

where d_{LF}^n is given in (6.7b) and

$$\text{(6.14b)}\quad d_\theta^n = (\Pi_h - \pi_h)(\!|\widetilde{u}^n|\!) + \pi_h \delta_\theta^n, \quad \delta_\theta^n = \delta_{4,0,+}^n + \delta_{4,0,-}^n - \tfrac{1}{4}\tau^2(\delta_{2,2,+}^n + \delta_{2,2,-}^n),$$

denotes the defect of the θ-scheme.

Proof. With the definition (3.7) of $\widehat{R}$, the identity $\langle\!\langle \widetilde{u}^n \rangle\!\rangle = \widetilde{u}^n + \frac{1}{4}(\!(\widetilde{u}^n)\!)$, and the consistency property (4.10), the defect d_h^n defined in (6.1) satisfies

$$\begin{aligned}\widehat{\mathbf{\Psi}}^{-1} d_h^n &= (I_h + \tfrac{1}{4}\tau^2 A_h\chi_m)\Pi_h(\!(\widetilde{u}^n)\!) - \tau^2(\tfrac{1}{4}A_h\Pi_h(\!(\widetilde{u}^n)\!) - A_h\Pi_h\langle\!\langle \widetilde{u}^n\rangle\!\rangle + \langle\!\langle f_h^n\rangle\!\rangle)\\ &= \Pi_h(\!(\widetilde{u}^n)\!) - \pi_h\tau^2\langle\!\langle \partial_t^2\widetilde{u}^n\rangle\!\rangle - \tfrac{1}{4}\tau^2 A_h\chi_e\Pi_h(\!(\widetilde{u}^n)\!).\end{aligned}$$

In the second step we additionally employed the differential equation (2.1) and the fact that $\chi_m + \chi_e \equiv 1$. The first two terms yield (6.14b) by Taylor expansion of $\delta_\theta^n = (\!(\widetilde{u}^n)\!) - \tau^2\langle\!\langle \partial_t^2\widetilde{u}^n\rangle\!\rangle$. For the third term we observe that by (6.8) we have

$$-\tfrac{1}{4}\tau^2 A_h\chi_e\Pi_h(\!(\widetilde{u}^n)\!) = -\tfrac{1}{4}\tau^2 A_h\chi_e\big((\Pi_h - \pi_h)(\!(\widetilde{u}^n)\!) + \pi_h\delta_{\mathrm{LF}}^n\big) - \tfrac{1}{4}\tau^4 A_h\chi_e\pi_h\partial_t^2\widetilde{u}^n,$$

which yields (6.14a) by multiplying with $\widehat{\mathbf{\Psi}}$. □

For the error of (3.5b)&(3.7) in the initial time step we have the following.

Lemma 6.7. *Let u be the solution of (2.1). If $u \in C(0,T;V_\star)\cap W^{3,1}(0,T;L^2(\Omega))$, then the defect d_h^0 of the starting value of the locally implicit scheme (3.5b)&(3.7) defined in (6.3) satisfies*

$$d_h^0 = \widehat{\mathbf{\Psi}} d_\theta^0 - \tfrac{1}{4}\tau^2\widehat{\mathbf{\Psi}} A_h\chi_e d_{\mathrm{LF}}^0 + \tfrac{1}{2}\Delta_{\mathrm{I}}^0, \tag{6.15a}$$

where

$$d_\theta^0 = (\Pi_h - \pi_h)(\widetilde{u}^1 - \widetilde{u}^0) + \pi_h(\delta_{3,0,+}^0 - \tfrac{1}{4}\tau^2\delta_{1,2,+}^0) \tag{6.15b}$$

and Δ_{I}^0 is defined as in Lemma 6.6.

Proof. Since for $\widehat{\mathbf{\Psi}} = \widehat{R}(\tau^2 A_h\chi_m)$

$$I_h - \tfrac{1}{4}\tau^2 A_h^{\Psi} = \widehat{\mathbf{\Psi}}\big(I_h - \tfrac{1}{4}\tau^2 A_h\chi_e\big),$$

we obtain from (6.3) with similar arguments as above for

$$\begin{aligned}\widehat{\mathbf{\Psi}}^{-1} d_h^0 &= (I_h + \tfrac{1}{4}\tau^2 A_h\chi_m)\Pi_h(\widetilde{u}^1 - \widetilde{u}^0) - \tau(I_h - \tfrac{1}{4}\tau^2 A_h\chi_e)v_h^0\\ &\quad - \tfrac{1}{2}\tau^2(-A_h\Pi_h\widetilde{u}^0 + \langle f_h^0\rangle)\\ &= \Pi_h(\widetilde{u}^1 - \widetilde{u}^0) - \pi_h(\tau v^0 + \tfrac{1}{2}\tau^2\langle\partial_t^2\widetilde{u}^0\rangle) - \tfrac{1}{4}\tau^2 A_h\chi_e\big(\Pi_h(\widetilde{u}^1 - \widetilde{u}^0) - \tau\pi_h v^0\big).\end{aligned}$$

Next, we use Taylor expansion. For the first two terms this yields (6.15b) and for the third term we have

$$-\tfrac{1}{4}\tau^2 A_h\chi_e\big(\Pi_h(\widetilde{u}^1 - \widetilde{u}^0) - \tau\pi_h v^0\big) = -\tfrac{1}{4}\tau^2 A_h\chi_e d_{\mathrm{LF}}^0 + \tfrac{1}{2}\widehat{\mathbf{\Psi}}^{-1}\Delta_{\mathrm{I}}^0.$$

Multiplying with $\widehat{\mathbf{\Psi}}$ leads to the formula for d_h^0. □

As mentioned before, if $\chi_e \equiv 0$ (i.e., all elements are treated implicitly), the defects in Lemmas 6.6 and 6.7 reduce to those of the θ-scheme. For the error result we now insert the defects d_h^n into the error representation (6.4) as we have done for the LTS scheme above. For the problematic terms – here consisting of the terms Δ_{I}^n – we apply Lemma 6.1 with

$$\Delta_*^n = \Delta_{\mathrm{I}}^n = -\tau^2\widehat{\mathbf{\Psi}} A_h\widetilde{\Delta}_{\mathrm{I}}^n, \qquad \widetilde{\Delta}_*^n = \widetilde{\Delta}_{\mathrm{I}}^n = \tfrac{1}{4}\tau^2\chi_e\pi_h\partial_t^2\widetilde{u}^n.$$

Altogether we obtain the error result.

Theorem 6.8. *Let $\sigma > \frac{1}{2}$, $\vartheta \in (0,1]$, $\tau \le \tau_{\mathrm{LI}}(\vartheta)$ defined in (5.7), and let Assumptions 2.2, 2.3, and 4.3 hold. Further, assume that the solution u of (2.1) satisfies the regularity assumptions (6.11). Then, for $t_n \le T$, the approximations u_h^n of the locally implicit scheme (3.5)&(3.7) with $\theta = \frac{1}{4}$ satisfy*

$$\|u(t_n) - u_h^n\| \le C \min\{c_{\mathrm{LI}}^{\vartheta}, t_n\}(\tau^2 + h^r), \qquad r = \min\{\sigma, k\} + \min\{\mu, 1\}, \tag{6.16}$$

where C only depends on C_R, θ, and u and its derivatives.

Proof. Combining (6.2) with Lemmas 6.6 and 6.7, Lemma 6.1 with $\Delta_*^n = \Delta_{\mathrm{I}}^n$, taking the norm, and using the stability estimates (5.8), (5.10) yields

$$\begin{aligned}\|e_h^n\| \le \|e_h^0\| &+ \min\{c_{\mathrm{LI}}^{\vartheta}, t_n\}\tfrac{1}{\tau}\Big(\|d_\theta^0\| + \sum\nolimits_{j=1}^{n-1}\|d_\theta^j\|\Big)\\ &+ \|\tfrac{1}{4}\tau^2 \boldsymbol{\mathcal{S}}_n^{\Psi}\widehat{\boldsymbol{\Psi}} A_h \chi_e d_{\mathrm{LF}}^0\| + \sum\nolimits_{j=1}^{n-1}\|\tfrac{1}{4}\tau^2 \boldsymbol{\mathcal{S}}_{n-j}^{\Psi}\widehat{\boldsymbol{\Psi}} A_h \chi_e d_{\mathrm{LF}}^j\|\\ &+ \|\widetilde{\Delta}_{\mathrm{I}}^n\| + \|\widetilde{\Delta}_{\mathrm{I}}^0\| + \min\{c_{\mathrm{LI}}^{\vartheta}, t_n\}\tfrac{1}{\tau}\Big(\|\widetilde{\Delta}_{\mathrm{I}}^1 - \widetilde{\Delta}_{\mathrm{I}}^0\| + \sum\nolimits_{j=1}^{n-1}\|\textcircled{\Delta}_{\mathrm{I}}^j\|\Big).\end{aligned}$$

The terms are bounded separately. The bound for e_h^0 is obvious. The defects d_θ^n can be estimated similarly as in the proof of the LTS scheme, leading to

$$\begin{aligned}\frac{1}{\tau}\Big(\|d_\theta^0\| + \sum\nolimits_{j=1}^{n-1}\|d_\theta^j\|\Big) &\le C_R \max_{s\in[0,\tau]} |\partial_t u(s)|_{r_*+1,\mathcal{T}_h}\, h^r + \tfrac{1}{4}\max_{s\in[0,\tau]}\|\partial_t^3 u(s)\|\,\tau^2\\ &\quad + C_R\int_0^{t_n} |\partial_t^2 u(s)|_{r_*+1,\mathcal{T}_h}\,\mathrm{d}s\, h^r + \tfrac{1}{6}\sqrt{2}\int_0^{t_n}\|\partial_t^4 u(s)\|\,\mathrm{d}s\,\tau^2.\end{aligned}$$

For the defects involving d_{LF}^j we observe that by the definition of $\boldsymbol{\mathcal{S}}_k^{\Psi}$ and because of $\widehat{\boldsymbol{\Psi}}\chi_e = \chi_e$ we have

$$\boldsymbol{\mathcal{S}}_{n-j}^{\Psi} A_h^{\Psi}\chi_e d_{\mathrm{LF}}^j = A_h^{\Psi}\boldsymbol{\mathcal{S}}_{n-j}^{\Psi}\widehat{\boldsymbol{\Psi}}\chi_e d_{\mathrm{LF}}^j.$$

Hence, the CFL condition (5.7) implies

$$\|\tfrac{1}{4}\tau^2 \boldsymbol{\mathcal{S}}_{n-j}^{\Psi}\widehat{\boldsymbol{\Psi}} A_h \chi_e d_{\mathrm{LF}}^j\| \le \tfrac{1}{\tau}\min\{c_{\mathrm{LI}}^{\vartheta}, t_n\}\|\chi_e d_{\mathrm{LF}}^j\|.$$

The bounds for $\|\chi_e d_{\mathrm{LF}}^j\|$ are the same as before. Moreover, again with Taylor expansion we have

$$\tfrac{1}{\tau}\Big(\|\widetilde{\Delta}_{\mathrm{I}}^1 - \widetilde{\Delta}_{\mathrm{I}}^0\| + \sum\nolimits_{j=1}^{n-1}\|\textcircled{\Delta}_{\mathrm{I}}^j\|\Big) \le \tfrac{1}{4}\Big(\max_{s\in[0,\tau]}\|\chi_e\partial_t^3 u(s)\| + 2\int_0^{t_n}\|\chi_e\partial_t^4 u(s)\|\,\mathrm{d}s\Big)\tau^2.$$

Collecting these bounds and inserting them into the first estimate yields the bound for $\|e_h^n\|$. The triangle inequality and Lemma 4.6 complete the proof. □

Note that with minor modifications the proof also holds for $\theta > \frac{1}{4}$.

6.3. **Extensions and generalizations.** We conclude this section with some notes about possible extensions of the local time integration schemes (and its error analysis) to other spatial discretizations and to more general problems than (2.1).

A close investigation of the stability and error analysis reveals that the precise structure of A_h is only used for bounds of the operators $A_{h,e}$, $A_{h,m}$, and $A_{h,em}$ in Appendix A, and thus for the CFL condition required for stability of the schemes. In fact, for the remaining analysis only the symmetry and consistency (4.10) of A_h are crucial. Moreover, the coercivity assumption of A_h can be weakened to A_h being non-negative by two minor modifications of the analysis:

(a) For the well-posedness, the elliptic projection (4.9) has to be constructed as in [24, Remark 32.16] which has the same properties as the stated one, in particular Lemmas 4.4 and 4.6 still hold.
(b) Since the stability bounds (5.9) and (5.10) do not hold anymore ((4.7) only holds with $\tilde{c}_{\mathrm{coer}} = 0$ under Assumption 4.3), we have $\min\{c^{\vartheta}_{\mathrm{LTS}}, t_n\} = \min\{c^{\vartheta}_{\mathrm{LI}}, t_n\} = t_n$ in the error bounds (6.12) and (6.16).

Hence, the analysis is extendable in several directions. First, instead of Dirichlet boundary conditions we can allow for Neumann or periodic boundary conditions resulting in a non-negative but not coercive A_h. Second, other discontinuous Galerkin space discretization methods for the operator A can be used as long as the resulting discrete operator A_h is symmetric, non-negative, and satisfies Lemmas 4.4 and 4.6. This is true, for instance, for the first, second, and fourth method in [4, Table 6.1]. Clearly, the bounds in Appendix A have to be verified for these variants. Moreover, depending on the chosen method, the submeshes $\mathcal{T}_{h,e}$ and $\mathcal{T}_{h,m}$ have to be selected slightly differently for efficiency reasons, e.g., for the local discontinuous Galerkin method [10].

Third, we could even consider more general linear second-order partial differential equations of the form

$$\partial_t^2 u + Au = f,$$

where A is self-adjoint and non-negative. By using a suitable discontinuous Galerkin space discretization for A, which again leads to a symmetric and non-negative discrete operator A_h, the error analysis can be performed in the same way. For example, the interior penalty discontinuous Galerkin method for Maxwell's equations fits into this setting; see, e.g., [31].

7. Numerical examples

In this section we present some numerical examples illustrating and confirming the previously shown theoretical results. We start with two simple one-dimensional examples before we turn towards two-dimensional problems. The codes for reproducing the numerical results are available on https://doi.org/10.5445/IR/1000158573. For an efficient implementation of the local time integration schemes we refer to [7]; see also [6, Section 5.6]. The spatial discretization in our codes is done with the software package FEniCS [41, 42].

For the LTS scheme an example with a discontinuous wave speed $\kappa^{1/2}$ can be found in [7, Section 6.3], further applications are given in [43] and [19, Section 5.2] with a slightly modified but unstabilized variant of the LTS scheme.

7.1. One-dimensional examples.

With the following two examples we confirm the necessity of choosing $\mathcal{T}_{h,m}$ as a true superset of $\mathcal{T}_{h,s}$ (by using an additional layer of one mesh element per face at the interface between $\mathcal{T}_{h,s}$ and $\mathcal{T}_{h,w}$) as well as the necessity of the stabilization parameter in the LTS methods to guarantee an enhanced stability behavior. For both examples we consider the wave equation (2.1) on $\Omega = (0,1)$ with $\kappa \equiv 1$. As initial values and for the right-hand side we use $u^0 = \sin(2\pi x)$, $v^0 \equiv 0$, and $f \equiv 0$, respectively, such that the exact solution is given by $u(t,x) = \sin(2\pi x)\cos(2\pi t)$. The simulation time is $T = 5$. For the space discretization we use polynomials of degree $k = 2$ as ansatz functions in the discrete space V_h and $\eta_S = 2$ as penalty parameter in the bilinear form (4.2).

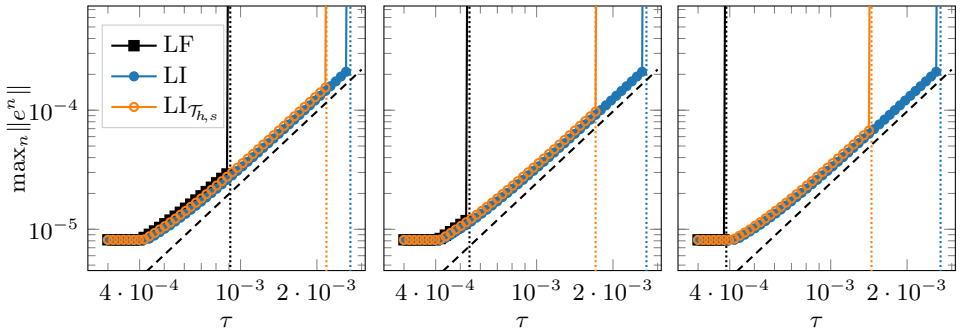

(a) $q = 3$. (b) $q = 5$. (c) $q = 7$.

FIGURE 1. Maximum error $\|e^n\|$ of the numerical solution over all timesteps for the leapfrog (LF) method, the locally implicit (LI) method, and the locally implicit method with $\mathcal{T}_{h,m} = \mathcal{T}_{h,s}$ (LI$_{\mathcal{T}_{h,s}}$). The dashed black lines indicate order two, the dotted vertical lines correspond to the theoretical CFL conditions of the leapfrog scheme if applied to the semidiscrete problem (3.1) on the meshes $\mathcal{T}_h$ (black), $\mathcal{T}_{h,w}$ (orange), and $\mathcal{T}_{h,e}$ (blue), respectively.

In the first example we use a set of three meshes $\mathcal{T}_h^q$, $q = 3, 5, 7$, consisting of a fixed equidistant coarse mesh $\mathcal{T}_{h,w}$ with $h_{\min,c} = 0.02$ and equidistant fine submeshes $\mathcal{T}_{h,s}^q$ satisfying $h_{\min,c}/h_{\min,f} = q$. In Figure 1 the errors of the leapfrog method and the locally implicit method are plotted against τ. For each mesh we apply the locally implicit method once with $\mathcal{T}_{h,m} = \mathcal{T}_{h,s}$ and once with $\mathcal{T}_{h,m}$ as defined in (4.11). Besides the second-order convergence in time we clearly observe that due to the CFL condition the maximal time-step size for which the leapfrog scheme is stable deteriorates with increasing q. A similar drift is visible for the locally implicit method, if $\mathcal{T}_{h,m} = \mathcal{T}_{h,s}$ is chosen. In contrast, for the correctly chosen $\mathcal{T}_{h,m}$ the examples confirm that the CFL condition of the locally implicit method is independent of the fine mesh $\mathcal{T}_{h,s}$. For the LTS scheme the same behavior as for the locally implicit method can be observed in numerical experiments.

In the second example the mesh $\mathcal{T}_h = \mathcal{T}_{h,w} \dot\cup \mathcal{T}_{h,s}$ consists of 108 mesh elements where $\mathcal{T}_{h,w}$ contains 106 elements of diameter $h_{\min,c} = 0.009375$ and $\mathcal{T}_{h,s}$ contains two elements of diameter $h_{\min,f} = h_{\min,c}/3$. To this problem we apply the leapfrog method and the LTS method with two different values for the stabilization parameter η. In Figure 2 the errors are plotted against the time-step size. Again, provided stability, we can clearly see the second-order convergence in time. Moreover, without stabilization, i.e., for $\eta = 0$, we observe that the LTS method becomes unstable at step sizes which are only up to $\pi/2$ larger than the maximum possible step size of the leapfrog scheme; cf. [7, Section 5]. Even a larger polynomial degree of the LFC polynomial (here for $p = 8$) does not overcome these shortcomings. In contrast, for $\eta = 0.1$ we observe that these instabilities vanish and the LTS scheme (if p is chosen appropriately) is stable for step sizes almost as large as the ones of the leapfrog scheme if applied to the semidiscrete problem (3.1) on the mesh $\mathcal{T}_{h,e}$.

7.2. **Two-dimensional examples.** For the two-dimensional example we consider the wave equation (2.1) on the square $\Omega = (-1, 1)^2$ again with a constant material

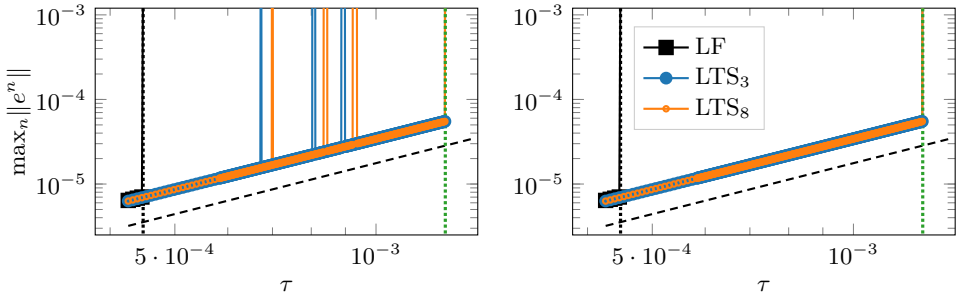

(a) $\eta = 0$. (b) $\eta = 0.1$.

FIGURE 2. Maximum error $\|e^n\|$ of the numerical solution over all timesteps for the leapfrog method (denoted with LF) and the LTS method with polynomial degree $p = 3$ (LTS_3) and $p = 8$ (LTS_8) for two values of the stabilization parameter η. The dashed black lines indicate order two, the dotted vertical lines correspond to the theoretical CFL conditions of the leapfrog scheme if applied to the semidiscrete problem (3.1) on the meshes $\mathcal{T}_h$ (black) and $\mathcal{T}_{h,e}$ (green), respectively.

parameter $\kappa \equiv 1$. The initial values and the right-hand side are chosen such that the exact solution is given by

$$u(t,x) = \sin(\pi x_1)\sin(\pi x_2)\big(\cos(\varpi t) + \sin(\varpi t)\big), \qquad \varpi = (2\pi^2 + 10)^{1/2}.$$

For the space discretization we use the meshes $\mathcal{T}_h^{j,\ell} = \mathcal{T}_{h,w}^j \cup \mathcal{T}_{h,s}^\ell$, $j, \ell \in \{1,2,3,4\}$, defined in [36]; see [36, fig. 1] for an illustration and also [50, Section 6.3.1]. The meshes $\mathcal{T}_{h,s}^\ell = \mathcal{T}_{h,f}^{(\ell)}$ representing the domain $(-0.5, 0.5)^2$ contain the small elements and $\mathcal{T}_{h,w}^j = \mathcal{T}_{h,c}^{(j)}$ contain the coarse ones. The data for the submeshes $\mathcal{T}_{h,w}^j$, $\mathcal{T}_{h,s}^\ell$ can be found in Appendix B.

As before, we use the penalty parameter $\eta_S = 2$ in the bilinear form (4.2). In all of the following plots the error $\|e^N\|$ is measured at time $t_N = 5$.

First, we look at the spatial convergence of the local time integration schemes. For this, we use the meshes $\mathcal{T}_h^{j,3}$, $j \in \{1,2,3,4\}$ with a fixed "fine" mesh. In Figure 3 the error is plotted against the mesh size h for the leapfrog, the locally implicit, and the LTS methods. Here, for the LFC polynomials in the LTS method, we fix the polynomial degree as $p = 16$ and the stabilization parameter as $\eta = 0.1$. For all three methods we observe the optimal order in space confirming our theoretical results. Moreover, the error constant for all methods almost coincide.

For the temporal convergence, we consider the meshes $\mathcal{T}_h^{j,\ell}$ with $j \in \{2,4\}$ and $\ell \in \{1,2,3,4\}$. As polynomial degree in space we employ $k = 3$. In Figure 4 the error is plotted against the time-step size τ. For the LFC polynomials P_p the stabilization parameter is again set to $\eta = 0.1$. The polynomial degree of P_p is chosen as $p = \lceil r \rceil$, where $r = \frac{\|A_h\|}{\|A_{h,e}\|}$. We clearly see that in contrast to the leapfrog method, the CFL condition of the locally implicit and the LTS method (with appropriately chosen p and η) is independent of the meshes $\mathcal{T}_{h,s}^\ell$ and only depends on the coarse meshes $\mathcal{T}_{h,w}^j$, $j \in \{2,4\}$. Moreover, all methods converge with order two in time with a constant independent of the spatial resolution confirming our theoretical results. In particular, for a fixed coarse mesh, the errors of the LTS

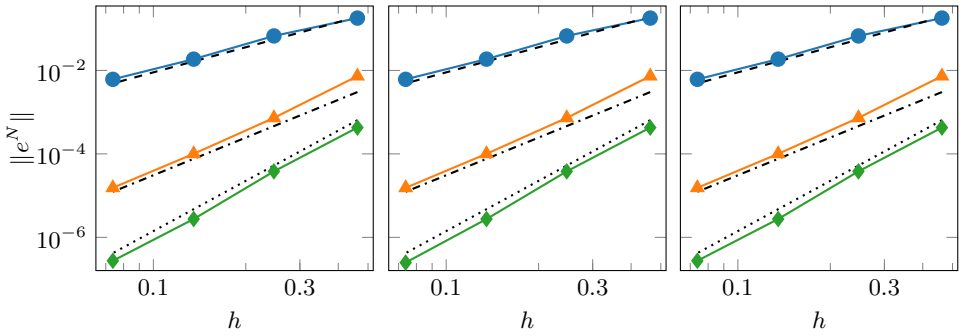

(a) leapfrog. (b) locally implicit. (c) LTS ($p = 16$, $\eta = 0.1$).

FIGURE 3. Error $\|e^N\|$ of the numerical solution at time $t_N = 5$ for the leapfrog, the locally implicit, and the LTS method ($p = 16$, $\eta = 0.1$) plotted against h with fixed time-step size $\tau = 10^{-4}$. The solid lines correspond to polynomial degree $k = 1$ (blue, circles), $k = 2$ (orange, triangles), $k = 3$ (green, rhombi) in the discrete space V_h. The black dashed, dash-dotted, and dotted line have slope h^{k+1} for $k = 1, 2, 3$, respectively.

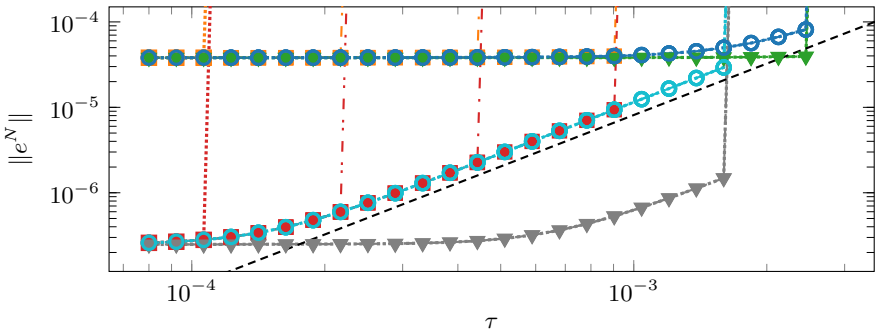

FIGURE 4. Error $\|e^N\|$ of the numerical solution at time $t_N = 5$ for the leapfrog, the locally implicit, and the LTS ($\eta = 0.1$) method plotted against τ for the meshes $\mathcal{T}_h^{j,\ell}$, $j \in \{2, 4\}$, $\ell \in \{1, 2, 3, 4\}$. The explanation of the markers, colors, and line styles are given in Table 1. The degree of the LFC polynomial P_p are chosen for each mesh as $p = \lceil r \rceil$, $r = \frac{\|A_h\|}{\|A_{h,e}\|}$. The black dashed line indicates order 2 in time. Note that the lines for different refinement levels ℓ are on top of each other.

TABLE 1. Legend for Figure 4.

	marker	$j = 2$	$j = 4$
leapfrog	square	orange	red
LTS	circle	blue	cyan
locally implicit	triangle	green	gray

ℓ	line style
1	dashed
2	dash-dotted
3	dash-dotdotted
4	dotted

and the locally implicit methods are for all four fine meshes approximately equal such that one cannot distinguish the corresponding lines in the figure. Interestingly, the locally implicit method has a much smaller error constant for the rather large norm of the inhomogeneity f used in this example.

Appendix A. Bounds for discrete operators

In this appendix, we show bounds for the operators $A_{h,m}$, $A_{h,e}$, and $A_{h,em}$ defined in (4.12) and (4.13), respectively. It is well-known that $\|A_h u_h\| \lesssim \xi_{\max}^2 \|u_h\|$ for $u_h \in V_h$, with $\xi_{\max}$ given in (3.3c); see, e.g., [32, Lemma 3.3] for a variant of the bilinear form a_h. However, to show the precise dependency of the bounds on the submeshes $\mathcal{T}_{h,b}$, $b \in \{w, s, e, m\}$, we state them here in detail. In addition to these bounds we also show an estimate for $\|A_h \chi_b u\|$, $u \in V_\star$, in Lemma A.2.

Notation. For the mesh faces $\mathcal{F}_h$ we use the partition

$$\mathcal{F}_h = \mathcal{F}_{h,e}^* \,\dot\cup\, \mathcal{F}_{h,m}\ , \qquad \mathcal{F}_{h,e}^* = \mathcal{F}_{h,e} \,\dot\cup\, \mathcal{F}_{h,em}.$$

Here, $\mathcal{F}_{h,e}$ and $\mathcal{F}_{h,m}$ contain the faces between or at the boundary of elements treated with the leapfrog and the modified scheme, respectively. The set $\mathcal{F}_{h,em} \subseteq \mathcal{F}_h^{\mathrm{int}}$ consists of the faces between the submeshes $\mathcal{T}_{h,e}$ and $\mathcal{T}_{h,m}$, i.e., a face $F \in \mathcal{F}_h^{\mathrm{int}}$ belongs to $\mathcal{F}_{h,em}$ if $F \subseteq \partial K_e \cap \partial K_m$ and $\mathrm{vol}_{d-1}(\partial K_e \cap \partial K_m) \neq 0$ for $K_e \in \mathcal{T}_{h,e}$, $K_m \in \mathcal{T}_{h,m}$. We use the convention that the normal n_F is directed from K_e towards K_m. From the shape-regularity of $\mathcal{T}_h$ (see Section 4.1) we further have that there is a constant $\rho_b > 0$ such that

$$\frac{h_K}{\delta_K} \le \rho_b \qquad \text{for all } K \in \mathcal{T}_{h,b}, \quad b \in \{w, s, e, m\}. \tag{A.1}$$

Note that $\rho \ge \rho_b$ and for locally refined meshes we might have $\rho \gg \rho_w$ in addition to $\xi_{\max} \gg \xi_{\max,w}$.

For proving the subsequent estimates the inverse and the discrete trace inequality for functions in V_h play a crucial role. For $u_h \in V_h$, the inverse inequality is given by

$$\|\nabla u_h\|_K \le C_{\mathrm{inv}} h_K^{-1} \|u_h\|_K \qquad \text{for all } K \in \mathcal{T}_h, \tag{A.2}$$

and the discrete trace inequality by

$$\|u_h\|_F \le C_{\mathrm{trc}} h_K^{-1/2} \|u_h\|_K \qquad \text{for all } F \in \mathcal{F}_h, K \in \mathcal{T}_h \text{ with } F \subset \partial K; \tag{A.3}$$

see, e.g., [18, Lemmas 1.44, 1.46]. Since the constants C_{inv} and C_{trc} depend on the shape-regularity constant ρ (and also the polynomial degree k of the finite element and the dimension d), we denote the corresponding constants on the submeshes $\mathcal{T}_{h,b}$ by $C_{\mathrm{inv},b}$ and $C_{\mathrm{trc},b}$ (depending on ρ_b, k and d).

The split operators $A_{h,m}$, $A_{h,e}$, and $A_{h,em}$ introduced in (4.12) are bounded as follows.

Lemma A.1. *For $u_h \in V_h$ we have*

$$\|A_{h,e} u_h\| = \|\chi_e A_h \chi_e u_h\| \le C_{\mathrm{bnd},w}\, \xi_{\max,w}^2 \|\chi_e u_h\|, \tag{A.4a}$$

$$\|A_{h,m} u_h\| = \|\chi_m A_h \chi_m u_h\| \le C_{\mathrm{bnd}}\, \xi_{\max}^2 \|\chi_m u_h\|, \tag{A.4b}$$

with $C_{\mathrm{bnd},w} = C_{\mathrm{inv},e}^2 + 2(\eta_S + C_{\mathrm{inv},e}) C_{\mathrm{trc},e}^2 \rho_w^2 N_\partial$, $C_{\mathrm{bnd}} = C_{\mathrm{inv}}^2 + 2(\eta_S + C_{\mathrm{inv}}) C_{\mathrm{trc}}^2 \rho^2 N_\partial$, *and*

$$\|A_{h,em} u_h\| = \|\chi_e A_h \chi_m u_h\| \le C_{\mathrm{bnd},w}^* \, \xi_{\max,w}^2 \|\chi_m u_h\| \tag{A.4c}$$

with $C_{\mathrm{bnd},w}^* = (\eta_S + C_{\mathrm{inv},w}) C_{\mathrm{trc},w}^2 \rho_w^2 N_\partial$.

Proof. We only show the bound (A.4a), the remaining ones can be proven analogously. Let $\varphi_h \in V_h$. Using the definitions of A_h in (4.6), a_h in (4.2), and of the indicator function χ_e in (3.4), we have

$$\begin{aligned}(\chi_e A_h \chi_e u_h, \varphi_h) = {} & \sum_{K \in \mathcal{T}_{h,e}} \int_K \kappa \nabla u_h \cdot \nabla \varphi_h \,\mathrm{d}x + \sum_{F \in \mathcal{F}_{h,e}^*} \mathrm{a}_F \int_F [\![\chi_e u_h]\!]_F [\![\chi_e \varphi_h]\!]_F \,\mathrm{d}\sigma \\ & - \sum_{F \in \mathcal{F}_{h,e}^*} \int_F \big(\{\!\{\kappa \nabla(\chi_e u_h)\}\!\}_F^{1/\kappa} \cdot n_F [\![\chi_e \varphi_h]\!]_F + \{\!\{\kappa \nabla(\chi_e \varphi_h)\}\!\}_F^{1/\kappa} \cdot n_F [\![\chi_e u_h]\!]_F \big) \,\mathrm{d}\sigma.\end{aligned}$$

The terms on the right-hand side are now bounded separately. For the first term we obtain with the Cauchy-Schwarz inequality, the inverse inequality (A.2), and the definition (3.2) of ξ_K

$$\sum_{K \in \mathcal{T}_{h,e}} \int_K \kappa \nabla u_h \cdot \nabla \varphi_h \,\mathrm{d}x \le C_{\mathrm{inv},e}^2 \sum_{K \in \mathcal{T}_{h,e}} \xi_K^2 \|u_h\|_K \|\varphi_h\|_K \le C_{\mathrm{inv},e}^2 \xi_{\max,w}^2 \|\chi_e u_h\| \|\varphi_h\|.$$

Next, for the penalty term, we again apply the Cauchy-Schwarz inequality twice

$$\begin{aligned}& \sum_{F \in \mathcal{F}_{h,e}^*} \mathrm{a}_F \int_F [\![\chi_e u_h]\!]_F [\![\chi_e \varphi_h]\!]_F \,\mathrm{d}\sigma \\ & \le \eta_S \Big(\sum_{F \in \mathcal{F}_{h,e}^*} \kappa_F^2 \, h_F^{-3} \|[\![\chi_e u_h]\!]_F\|_F^2 \Big)^{1/2} \Big(\sum_{F \in \mathcal{F}_{h,e}^*} h_F \|[\![\chi_e \varphi_h]\!]_F\|_F^2 \Big)^{1/2}.\end{aligned}$$

Since both factors are bounded by similar arguments, we only show the bound for the first one. For this, we first observe that by the definition (4.3) of h_F together with the shape-regularity (A.1)

$$h_F \le h_{K_{F,1}}, h_{K_{F,2}} \le \rho_w h_F \qquad \text{for all } F \in \mathcal{F}_{h,e}^* \cap \mathcal{F}_h^{\mathrm{int}}, F = \partial K_{F,1} \cap \partial K_{F,2}, \tag{A.5}$$

and by the definition (4.4) of κ_F

$$\kappa_F \le \max\{\kappa_{K_{F,1}}, \kappa_{K_{F,2}}\} \qquad \text{for all } F \in \mathcal{F}_h^{\mathrm{int}}, F = \partial K_{F,1} \cap \partial K_{F,2}. \tag{A.6}$$

Thus, we have for all $F \in \mathcal{F}_{h,e} \cap \mathcal{F}_h^{\mathrm{int}}$

$$\begin{aligned}\kappa_F^2 \, h_F^{-3} \|[\![u_h]\!]_F\|_F^2 &\le 2 C_{\mathrm{trc},e}^2 \kappa_F^2 \, h_F^{-3} \big(h_{K_{F,1}}^{-1} \|u_h\|_{K_{F,1}}^2 + h_{K_{F,2}}^{-1} \|u_h\|_{K_{F,2}}^2 \big) \\ &\le 2 C_{\mathrm{trc},e}^2 \, \rho_w^4 \, \max\{\xi_{K_{F,1}}, \xi_{K_{F,2}}\}^4 \big(\|u_h\|_{K_{F,1}}^2 + \|u_h\|_{K_{F,2}}^2 \big),\end{aligned}$$

where we additionally used the discrete trace inequality (A.3) in the first step. Proceeding similarly for $F \in \mathcal{F}_{h,e} \cap \mathcal{F}_h^{\mathrm{bnd}}$ and $F \in \mathcal{F}_{h,em}$ (note that $[\![\chi_e u_h]\!]_F = (u_h|_{K_e})|_F$ for all $F \in \mathcal{F}_{h,em}$) yields together with the definition of N_∂

$$\sum_{F \in \mathcal{F}_{h,e}^*} \mathrm{a}_F \int_F [\![\chi_e u_h]\!]_F [\![\chi_e \varphi_h]\!]_F \,\mathrm{d}\sigma \le 2 \eta_S \, C_{\mathrm{trc},e}^2 N_\partial \rho_w^2 \xi_{\max,w}^2 \|\chi_e u_h\| \|\varphi_h\|.$$

For the consistency and symmetry terms we observe that by the definition of the weighted average (4.1) we have for all $F \in \mathcal{F}_{h,e} \cap \mathcal{F}_h^{\mathrm{int}}$

$$\begin{aligned} h_F^{-1}\|\{\!\{\kappa\nabla u_h\}\!\}_F^{1/\kappa}\|_F^2 &\le \tfrac{1}{2}\kappa_F^2\Big(\|\nabla u_h|_{K_{F,1}}\|_F^2 + \|\nabla u_h|_{K_{F,2}}\|_F^2\Big) \\ &\le \tfrac{1}{2}C_{\mathrm{trc},e}^2 C_{\mathrm{inv},e}^2 \kappa_F^2\, h_F^{-1}\big(h_{K_{F,1}}^{-3}\|u_h\|_{K_{F,1}}^2 + h_{K_{F,2}}^{-3}\|u_h\|_{K_{F,2}}^2\big) \\ &\le \tfrac{1}{2}C_{\mathrm{trc},e}^2 C_{\mathrm{inv},e}^2\, \rho_w^4\, \max\{\xi_{K_{F,1}},\xi_{K_{F,2}}\}^4\Big(\|u_h\|_{K_{F,1}}^2 + \|u_h\|_{K_{F,2}}^2\Big), \end{aligned}$$

where we again used (A.5), (A.6), (A.3), and (A.2). Thus, using similar arguments as for the penalty term leads to

$$\begin{aligned} &\sum_{F\in\mathcal{F}_{h,e}^*}\int_F \big(\{\!\{\kappa\nabla(\chi_e u_h)\}\!\}_F^{1/\kappa}\cdot n_F[\![\chi_e\varphi_h]\!]_F + \{\!\{\kappa\nabla(\chi_e\varphi_h)\}\!\}_F^{1/\kappa}\cdot n_F[\![\chi_e u_h]\!]_F\big)\,\mathrm{d}\sigma \\ &\quad\le 2\,C_{\mathrm{trc},e}^2 C_{\mathrm{inv},e} N_\partial\,\rho_w^2\,\xi_{\max,w}^2\|\chi_e u_h\|\|\varphi_h\|. \end{aligned}$$

Collecting the estimates of all terms and using the identity

$$\|\chi_e A_h \chi_e u_h\| = \sup_{\varphi_h\in V_h,\|\varphi_h\|=1}(\chi_e A_h\chi_e u_h,\varphi_h)$$

finishes the proof. □

The next lemma states that $\|A_h\chi_b u\|$, $b\in\{e,m\}$, cannot be uniformly bounded in h (or $h_{\min}$) for functions $u\in V_\star$.

Lemma A.2. *For $u\in V_\star$ and $b\in\{e,m\}$ we have*

$$\begin{aligned} \|A_h\chi_b u\| &\le \Big(\sum_{K\in\mathcal{T}_{h,b}}\|Au\|_K^2\Big)^{1/2} + C_{\mathrm{or},c}\kappa_{\max,w}\Big(\sum_{F\in\mathcal{F}_{h,em}} h_F^{-3}\,\|u\|_F^2\Big)^{1/2} \\ &\quad + \sqrt{2}\,C_{\mathrm{trc},w}N_\partial^{1/2}\kappa_{\max,w}\Big(\sum_{F\in\mathcal{F}_{h,em}} h_F^{-1}\,\|\nabla u\|_F^2\Big)^{1/2} \end{aligned} \tag{A.7}$$

with $C_{\mathrm{or},c} = (2\eta_S + C_{\mathrm{inv},w})C_{\mathrm{trc},w}N_\partial^{1/2}$ and $\kappa_{\max,w} = \max_{K\in\mathcal{T}_{h,w}}\kappa_K$.

Proof. Let $\varphi_h\in V_h$. Since $u\in V_\star$, we have $\chi_b u\in V_{\star,h}$ as well as $[\![u]\!]_F = 0$ for all $F\in\mathcal{F}_h\setminus\mathcal{F}_{h,em}$ and $[\![\kappa\nabla u]\!]_F = 0$ for all $F\in\mathcal{F}_h^{\mathrm{int}}\setminus\mathcal{F}_{h,em}$. Elementwise integration by parts then yields for all $\varphi_h\in V_h$

$$\begin{aligned} (A_h\chi_b u,\varphi_h) &= a_h(\chi_b u,\varphi_h) \\ &= -\sum_{K\in\mathcal{T}_{h,b}}\int_K \nabla\cdot(\kappa\nabla u)\varphi_h\,\mathrm{d}x + \sum_{F\in\mathcal{F}_{h,em}}\mathrm{a}_F\int_F [\![\chi_b u]\!]_F[\![\varphi_h]\!]_F\,\mathrm{d}\sigma \\ &\quad + \sum_{F\in\mathcal{F}_{h,em}}\int_F\big([\![\kappa\nabla(\chi_b u)]\!]_F\cdot n_F\{\!\{\varphi_h\}\!\}_F^\kappa - \{\!\{\kappa\nabla(\varphi_h)\}\!\}_F^{1/\kappa}\cdot n_F[\![\chi_b u]\!]_F\big)\,\mathrm{d}\sigma. \end{aligned}$$

Similar arguments as in the previous proof lead to (A.7). □

Appendix B. Mesh data

In Table 2 we collect the data of the submeshes $\mathcal{T}_{h,w}^j$, $\mathcal{T}_{h,s}^\ell$, $j,\ell\in\{1,2,3,4\}$, which build the meshes $\mathcal{T}_h^{j,\ell} = \mathcal{T}_{h,w}^j\cup\mathcal{T}_{h,s}^\ell$ used in Section 7.2. Here, we denote

$$h_{\min,b}^{(a)} = \min_{K\in\mathcal{T}_{h,b}^a} h_K,\quad h_{\max,b}^{(a)} = \max_{K\in\mathcal{T}_{h,b}^a} h_K,\qquad (a,b)\in\big\{(j,w),(\ell,s)\big\}.$$

TABLE 2. Data of the submeshes $\mathcal{T}_{h,w}^{j}$, $\mathcal{T}_{h,s}^{\ell}$, $j, \ell \in \{1,2,3,4\}$.

(a) $\mathcal{T}_{h,w}^{j}$.

j	$h_{\max,w}^{(j)}$	$h_{\min,w}^{(j)}$	#elements
1	0.4618	0.0625	188
2	0.2469	0.05	528
3	0.1353	0.05	1448
4	0.0738	0.0373	3992

(b) $\mathcal{T}_{h,s}^{\ell}$.

ℓ	$h_{\max,s}^{(\ell)}$	$h_{\min,s}^{(\ell)}$	#elements
1	0.05	0.025	32
2	0.05	0.0125	48
3	0.05	0.00625	64
4	0.05	0.003125	80

ACKNOWLEDGMENTS

We thank Raphael Adalid Braun, Benjamin Dörich, and Vera Hugler for their careful reading of this manuscript.

REFERENCES

[1] M. ABRAMOWITZ AND I. A. STEGUN, *Handbook of mathematical functions with formulas, graphs, and mathematical tables*, National Bureau of Standards Applied Mathematics Series, No. 55, U. S. Government Printing Office, Washington, D.C., 1964. For sale by the Superintendent of Documents.

[2] R. A. ADAMS AND J. J. F. FOURNIER, *Sobolev spaces*, vol. 140 of Pure and Applied Mathematics (Amsterdam), Elsevier/Academic Press, Amsterdam, second ed., 2003.

[3] M. ALMQUIST AND M. MEHLIN, *Multilevel local time-stepping methods of Runge-Kutta-type for wave equations*, SIAM J. Sci. Comput., 39 (2017), pp. A2020–A2048, https://doi.org/10.1137/16M1084407.

[4] D. N. ARNOLD, F. BREZZI, B. COCKBURN, AND L. D. MARINI, *Unified analysis of discontinuous Galerkin methods for elliptic problems*, SIAM J. Numer. Anal., 39 (2001/02), pp. 1749–1779, https://doi.org/10.1137/S0036142901384162.

[5] S. C. BRENNER, *Poincaré-Friedrichs inequalities for piecewise H^1 functions*, SIAM J. Numer. Anal., 41 (2003), pp. 306–324, https://doi.org/10.1137/S0036142902401311.

[6] C. CARLE, *On leapfrog-Chebyshev schemes for second-order differential equations*, PhD thesis, Karlsruhe Institute of Technology (KIT), 2021, https://doi.org/10.5445/IR/1000147725.

[7] C. CARLE AND M. HOCHBRUCK, *Error Analysis of Multirate Leapfrog-Type Methods for Second-Order Semilinear Odes*, SIAM J. Numer. Anal., 60 (2022), pp. 2897–2924, https://doi.org/10.1137/21M1427255.

[8] C. CARLE, M. HOCHBRUCK, AND A. STURM, *On leapfrog-Chebyshev schemes*, SIAM J. Numer. Anal., 58 (2020), pp. 2404–2433, https://doi.org/10.1137/18M1209453.

[9] J. CHABASSIER AND S. IMPERIALE, *Construction and convergence analysis of conservative second order local time discretisation for linear wave equations*, ESAIM Math. Model. Numer. Anal., 55 (2021), pp. 1507–1543, https://doi.org/10.1051/m2an/2021030.

[10] B. COCKBURN AND C.-W. SHU, *The local discontinuous Galerkin method for time-dependent convection-diffusion systems*, SIAM J. Numer. Anal., 35 (1998), pp. 2440–2463, https://doi.org/10.1137/S0036142997316712.

[11] F. COLLINO, T. FOUQUET, AND P. JOLY, *A conservative space-time mesh refinement method for the 1-D wave equation. I. Construction*, Numer. Math., 95 (2003), pp. 197–221, https://doi.org/10.1007/s00211-002-0446-5.

[12] F. COLLINO, T. FOUQUET, AND P. JOLY, *A conservative space-time mesh refinement method for the 1-D wave equation. II. Analysis*, Numer. Math., 95 (2003), pp. 223–251, https://doi.org/10.1007/s00211-002-0447-4.

[13] M. COSTABEL, M. DAUGE, AND S. NICAISE, *Singularities of Maxwell interface problems*, M2AN Math. Model. Numer. Anal., 33 (1999), pp. 627–649, https://doi.org/10.1051/m2an:1999155.

[14] S. DESCOMBES, S. LANTERI, AND L. MOYA, *Locally implicit time integration strategies in a discontinuous Galerkin method for Maxwell's equations*, J. Sci. Comput., 56 (2013), pp. 190–218, https://doi.org/10.1007/s10915-012-9669-5.

[15] S. Descombes, S. Lanteri, and L. Moya, *High-order locally implicit time integration strategies in a discontinuous Galerkin method for Maxwell's equations*, in Spectral and high order methods for partial differential equations—ICOSAHOM 2012, vol. 95 of Lect. Notes Comput. Sci. Eng., Springer, Cham, 2014, pp. 205–215, https://doi.org/10.1007/978-3-319-01601-6_16.

[16] S. Descombes, S. Lanteri, and L. Moya, *Temporal convergence analysis of a locally implicit discontinuous Galerkin time domain method for electromagnetic wave propagation in dispersive media*, J. Comput. Appl. Math., 316 (2017), pp. 122–132, https://doi.org/10.1016/j.cam.2016.09.038.

[17] E. Di Nezza, G. Palatucci, and E. Valdinoci, *Hitchhiker's guide to the fractional Sobolev spaces*, Bull. Sci. Math., 136 (2012), pp. 521–573, https://doi.org/10.1016/j.bulsci.2011.12.004.

[18] D. A. Di Pietro and A. Ern, *Mathematical aspects of discontinuous Galerkin methods*, vol. 69 of Mathématiques & Applications (Berlin) [Mathematics & Applications], Springer, Heidelberg, 2012, https://doi.org/10.1007/978-3-642-22980-0.

[19] J. Diaz and M. J. Grote, *Energy conserving explicit local time stepping for second-order wave equations*, SIAM J. Sci. Comput., 31 (2009), pp. 1985–2014, https://doi.org/10.1137/070709414.

[20] J. Diaz and M. J. Grote, *Multi-level explicit local time-stepping methods for second-order wave equations*, Comput. Methods Appl. Mech. Engrg., 291 (2015), pp. 240–265, https://doi.org/10.1016/j.cma.2015.03.027.

[21] V. Dolean, H. Fahs, L. Fezoui, and S. Lanteri, *Locally implicit discontinuous Galerkin method for time domain electromagnetics*, J. Comput. Phys., 229 (2010), pp. 512–526, https://doi.org/10.1016/j.jcp.2009.09.038.

[22] M. Dryja, *On discontinuous Galerkin methods for elliptic problems with discontinuous coefficients*, Comput. Methods Appl. Math., 3 (2003), pp. 76–85, https://doi.org/10.2478/cmam-2003-0007. Dedicated to Raytcho Lazarov.

[23] A. Ern and J.-L. Guermond, *Finite elements I—Approximation and interpolation*, vol. 72 of Texts in Applied Mathematics, Springer, Cham, [2021] ©2021, https://doi.org/10.1007/978-3-030-56341-7.

[24] A. Ern and J.-L. Guermond, *Finite elements II—Galerkin approximation, elliptic and mixed PDEs*, vol. 73 of Texts in Applied Mathematics, Springer, Cham, [2021] ©2021, https://doi.org/10.1007/978-3-030-56923-5.

[25] M. Grote, S. Michel, and S. Sauter, *Stabilized leapfrog based local time-stepping method for the wave equation*, Math. Comp., 90 (2021), pp. 2603–2643, https://doi.org/10.1090/mcom/3650.

[26] M. J. Grote, M. Mehlin, and T. Mitkova, *Runge-Kutta-based explicit local time-stepping methods for wave propagation*, SIAM J. Sci. Comput., 37 (2015), pp. A747–A775, https://doi.org/10.1137/140958293.

[27] M. J. Grote and T. Mitkova, *Explicit local time-stepping methods for Maxwell's equations*, J. Comput. Appl. Math., 234 (2010), pp. 3283–3302, https://doi.org/10.1016/j.cam.2010.04.028.

[28] M. J. Grote and T. Mitkova, *Explicit local time-stepping methods for time-dependent wave propagation*, in Direct and inverse problems in wave propagation and applications, vol. 14 of Radon Ser. Comput. Appl. Math., De Gruyter, Berlin, 2013, pp. 187–218, https://doi.org/10.1515/9783110282283.187.

[29] M. J. Grote and T. Mitkova, *High-order explicit local time-stepping methods for damped wave equations*, J. Comput. Appl. Math., 239 (2013), pp. 270–289, https://doi.org/10.1016/j.cam.2012.09.046.

[30] M. J. Grote, A. Schneebeli, and D. Schötzau, *Discontinuous Galerkin finite element method for the wave equation*, SIAM J. Numer. Anal., 44 (2006), pp. 2408–2431, https://doi.org/10.1137/05063194X.

[31] M. J. Grote, A. Schneebeli, and D. Schötzau, *Interior penalty discontinuous Galerkin method for Maxwell's equations: optimal L^2-norm error estimates*, IMA J. Numer. Anal., 28 (2008), pp. 440–468, https://doi.org/10.1093/imanum/drm038.

[32] M. J. Grote and D. Schötzau, *Optimal error estimates for the fully discrete interior penalty DG method for the wave equation*, J. Sci. Comput., 40 (2009), pp. 257–272, https://doi.org/10.1007/s10915-008-9247-z.

[33] E. Hairer, C. Lubich, and G. Wanner, *Geometric numerical integration*, vol. 31 of Springer Series in Computational Mathematics, Springer-Verlag, Berlin, second ed., 2006, https://doi.org/10.1007/3-540-30666-8. Structure-preserving algorithms for ordinary differential equations.

[34] D. Hipp, M. Hochbruck, and C. Stohrer, *Unified error analysis for nonconforming space discretizations of wave-type equations*, IMA J. Numer. Anal., 39 (2019), pp. 1206–1245, https://doi.org/10.1093/imanum/dry036.

[35] D. Hipp and B. Kovács, *Finite element error analysis of wave equations with dynamic boundary conditions: L^2 estimates*, IMA J. Numer. Anal., 41 (2021), pp. 683–728, https://doi.org/10.1093/imanum/drz073.

[36] M. Hochbruck and A. Sturm, *Error analysis of a second-order locally implicit method for linear Maxwell's equations*, SIAM J. Numer. Anal., 54 (2016), pp. 3167–3191, https://doi.org/10.1137/15M1038037.

[37] M. Hochbruck and A. Sturm, *Upwind discontinuous Galerkin space discretization and locally implicit time integration for linear Maxwell's equations*, Math. Comp., 88 (2019), pp. 1121–1153, https://doi.org/10.1090/mcom/3365.

[38] P. Joly and J. Rodríguez, *An error analysis of conservative space-time mesh refinement methods for the one-dimensional wave equation*, SIAM J. Numer. Anal., 43 (2005), pp. 825–859, https://doi.org/10.1137/040603437.

[39] S. Karaa, *Finite element θ-schemes for the acoustic wave equation*, Adv. Appl. Math. Mech., 3 (2011), pp. 181–203, https://doi.org/10.4208/aamm.10-m1018.

[40] M. Kotovshchikova, D. K. Firsov, and S. H. Lui, *A third-order multirate Runge-Kutta scheme for finite volume solution of 3D time-dependent Maxwell's equations*, Commun. Appl. Math. Comput. Sci., 15 (2020), pp. 65–87, https://doi.org/10.2140/camcos.2020.15.65.

[41] A. Logg, K.-A. Mardal, and G. N. Wells, eds., *Automated solution of differential equations by the finite element method*, vol. 84 of Lecture Notes in Computational Science and Engineering, Springer, Heidelberg, 2012, https://doi.org/10.1007/978-3-642-23099-8. The FEniCS book.

[42] A. Logg and G. N. Wells, *DOLFIN: automated finite element computing*, ACM Trans. Math. Software, 37 (2010), pp. Art. 20, 28, https://doi.org/10.1145/1731022.1731030, https://doi.org/10.1145/1731022.1731030.

[43] S. Minisini, E. Zhebel, A. Kononov, and W. A. Mulder, *Local time stepping with the discontinuous galerkin method for wave propagation in 3d heterogeneous media*, GEOPHYSICS, 78 (2013), pp. T67–T77, https://doi.org/10.1190/geo2012-0252.1.

[44] E. Montseny, S. Pernet, X. Ferriéres, and G. Cohen, *Dissipative terms and local time-stepping improvements in a spatial high order discontinuous Galerkin scheme for the time-domain Maxwell's equations*, J. Comput. Phys., 227 (2008), pp. 6795–6820, https://doi.org/10.1016/j.jcp.2008.03.032.

[45] F. Müller and C. Schwab, *Finite elements with mesh refinement for elastic wave propagation in polygons*, Math. Methods Appl. Sci., 39 (2016), pp. 5027–5042, https://doi.org/10.1002/mma.3355.

[46] S. Nicaise, *Polygonal interface problems*, vol. 39 of Methoden und Verfahren der Mathematischen Physik [Methods and Procedures in Mathematical Physics], Verlag Peter D. Lang, Frankfurt am Main, 1993.

[47] M. Petzoldt, *Regularity results for Laplace interface problems in two dimensions*, Z. Anal. Anwendungen, 20 (2001), pp. 431–455, https://doi.org/10.4171/ZAA/1024.

[48] S. Piperno, *Symplectic local time-stepping in non-dissipative DGTD methods applied to wave propagation problems*, M2AN Math. Model. Numer. Anal., 40 (2006), pp. 815–841 (2007), https://doi.org/10.1051/m2an:2006035.

[49] T. Rylander and A. Bondeson, *Stability of explicit–implicit hybrid time-stepping schemes for Maxwell's equations*, J. Comput. Phys., 179 (2002), pp. 426–438, https://doi.org/https://doi.org/10.1006/jcph.2002.7063.

[50] A. Sturm, *Locally implicit time integration for linear Maxwells equations*, PhD thesis, Karlsruhe Institute of Technology (KIT), 2017, http://dx.doi.org/10.5445/IR/1000069341.

[51] L. Tartar, *An introduction to Sobolev spaces and interpolation spaces*, vol. 3 of Lecture Notes of the Unione Matematica Italiana, Springer, Berlin; UMI, Bologna, 2007, https://doi.org/10.1007/978-3-540-71483-5.

[52] J. G. Verwer, *Component splitting for semi-discrete Maxwell equations*, BIT, 51 (2011), pp. 427–445, https://doi.org/10.1007/s10543-010-0296-y.

Institute for Applied and Numerical Mathematics, Karlsruhe Institute of Technology, Englerstr. 2, 76131 Karlsruhe, Germany
Email address: constantin.carle@kit.edu

Institute for Applied and Numerical Mathematics, Karlsruhe Institute of Technology, Englerstr. 2, 76131 Karlsruhe, Germany
Email address: marlis.hochbruck@kit.edu